

Tensor Comprehensions: Framework-Agnostic High-Performance Machine Learning Abstractions

Nicolas Vasilache

Facebook AI Research
ntv@fb.com

Oleksandr Zinenko

Inria & ENS, DI
oleksandr.zinenko@inria.fr

Theodoros Theodoridis

ETH Zürich
theodort@student.ethz.ch

Priya Goyal

Facebook AI Research
prigoyal@fb.com

Zachary DeVito

Facebook AI Research
zdevito@fb.com

William S. Moses

MIT CSAIL
wmoses@mit.edu

Sven Verdoolaege

Polly Labs & Facebook AI Research
sven.verdoolaege@gmail.com

Andrew Adams

Facebook AI Research
andrew.b.adams@gmail.com

Albert Cohen

Inria & ENS, DI & Facebook AI Research
albert.cohen@inria.fr

Abstract

Deep learning models with convolutional and recurrent networks are now ubiquitous and analyze massive amounts of audio, image, video, text and graph data, with applications in automatic translation, speech-to-text, scene understanding, ranking user preferences, ad placement, etc. Competing frameworks for building these networks such as TensorFlow, Chainer, CNTK, Torch/PyTorch, Caffe1/2, MXNet and Theano, explore different tradeoffs between usability and expressiveness, research or production orientation and supported hardware. They operate on a DAG of computational operators, wrapping high-performance libraries such as CUDNN (for NVIDIA GPUs) or NNPACK (for various CPUs), and automate memory allocation, synchronization, distribution. Custom operators are needed where the computation does not fit existing high-performance library calls, usually at a high engineering cost. This is frequently required when new operators are invented by researchers: such operators suffer a severe performance penalty, which limits the pace of innovation. Furthermore, even if there is an existing runtime call these frameworks can use, it often does not offer optimal performance for a user's particular network architecture and dataset, missing optimizations between operators as well as optimizations that can be done knowing the size and shape of data. Our contributions include (1) a language close to the mathematics of deep learning called *Tensor Comprehensions*, (2) a polyhedral Just-In-Time compiler to convert a mathematical description of a deep learning DAG into a CUDA kernel with delegated memory management and synchronization, also providing optimizations such as operator fusion and specialization for specific sizes, (3) a compilation cache populated by an autotuner. In particular, we demonstrate the suitability of the polyhedral framework to construct a domain-specific optimizer effective on state-of-the-art deep learning models on GPUs. Our flow reaches up to $4\times$ speedup over NVIDIA libraries on kernels relevant to the Machine Learning Community, and on an actual model used in production at Facebook. It is integrated with mainstream frameworks Caffe2 (production-oriented), PyTorch (research-oriented), through the ATen asynchronous tensor library.

1 Introduction

Deep neural networks trained with back-propagation learning [52] are a method of choice to solve complex problems with sufficient data. Recently, GPU-accelerated algorithms have excelled in this area [73, 21, 50]. Popular computation graph engines [81, 24, 17, 1] offer high-level abstractions for optimizing and executing deep neural networks expressed as graphs of tensor operations. These frameworks make transparent use of GPUs and other hardware accelerators for low power or low latency [55, 44] and are often implemented as an abstraction over highly-optimized routines for individual operators. While these operators are sufficient for many applications, they fall short in a number of instances where the computation does not fit the supported library calls. Consider a researcher who wants to develop a novel type of layer or network architecture. She must develop a custom operator, often at a high engineering cost and performance penalty. Furthermore, even when it is possible to represent a given network with library calls, they often miss peak performance for two reasons: missed optimizations across operators, and no tuning for every combination of size, shape and data flow encountered in Machine Learning (ML) [83].

Alone, computation graphs in such frameworks are too abstract to capture essential refinements and lowering steps required for efficient use of hardware accelerators, unless the operators perfectly fit a pre-optimized set of library functions. The parallel execution of individual layers and the memory layout of individual tensors varies greatly depending on data size and shape, upstream and downstream computations, and specific hardware features.

1.1 Motivations

These observations have pushed for an active library [85, 8] or built-to-order (BTO) approach [9], in which library code is specialized and generated on-demand. However, this approach does not quite solve the problem as tuning library kernels in isolation misses context-dependent opportunities and creating a library that covers all combinations of individual kernels is infeasible.

This has led to the creation of domain-specific languages such as Halide [72], which has been successful in imaging due to its ability to fuse large pipelines without obfuscating the underlying algorithm. However when using Halide on the GPU, all scheduling transformations must be manually specified, and achieving high performance with the right combination of them is beyond the ability of most users.

More recent deep learning compilers such as XLA [36] and Latte [82] seem to be the ideal solution to this problem: they combine operators from computation graphs, allowing for optimizations across operators as well as optimizations that take advantage of data size. Yet, so far, the expected performance levels have not been met on GPU targets. The transformation language of these frameworks does not seem to be able to represent complex scheduling and mapping transformations which are often crucial to GPU targets with partitioned memory architectures.

To remedy this, an effective programming language for computation graph engines must simultaneously address the two following challenges:

- ensure that abstraction not only enhances programmer productivity but also enables the compiler and its supporting execution environment to eliminate concerns irrelevant to the target platform, to refine the code through intermediate representations closer to the machine, and to automatically explore a wide optimization space. In other words, the system must be able to offer “abstraction without regret” [76, 22] while conveying rich semantical information available at compilation time;
- select appropriate intermediate representations and optimization algorithms that deal with deep parallelism and memory hierarchies, as well as hardware features such as vector instructions and special-purpose memory.

1.2 Contributions

We present a novel domain-specific flow capable of generating highly-optimized kernels for tensor expressions, leveraging optimizations across operators and optimizations that take into account the size and shape of data. We address the first challenge through the design of Tensor Comprehensions (TC), a domain-specific language whose syntax is both concise and expressive and whose

semantics allows for efficient memory management and mapping to complex parallel platforms. We address the second challenge by specializing a polyhedral intermediate representation and its compilation algorithms to the domain of deep learning, providing it with a dedicated autotuner. The polyhedral framework of compilation emerged as a natural candidate to design a versatile intermediate representation and optimization flow satisfying the needs of the domain and target hardware. The polyhedral framework has demonstrated strong results in domain-specific optimization [59, 7, 3], expert-driven metaprogramming [32, 15, 4], libraries of high-level transformations of control flow and storage [48], and embedding of third-party library code [49], and automatic generation of efficient code for heterogeneous targets [5, 54, 66, 88, 3, 95].

In this report, we present the following contributions:

- Tensor Comprehensions (TC): a high-level language to express tensor computations arising in ML with a syntax generalizing the Einstein notation. It supports shape and size inference, flexible element-wise syntax with both named and positional parameters. It has conciseness and safety advantages, avoiding off-by-one errors while also allowing layout transformations and specialization.
- An end-to-end compilation flow capable of lowering tensor comprehensions to efficient GPU code. It delivers strong baseline performance for custom operators and remains competitive with vendor libraries on standard ones. The former is essential to reducing the technical debt on vendor libraries, enabling ML researchers to explore a wider field of architectures and layers in production-like scenarios.
- A collection of polyhedral compilation algorithms with a specific domain and target orientation. Unlike general-purpose parallelizing compilers, we primarily optimize for reduced launch and synchronization overhead through kernel fusion and also favor multi-level parallelism and promotion to deeper levels of the memory hierarchy.
- An autotuning framework that takes advantage of Just-In-Time (JIT) compilation and code caching. It includes specialization for non-standard sizes, eliminating control and address generation logic, and takes ownership of all optimization knobs from the ML framework to the code generator.
- Integration into two common ML frameworks (PyTorch [71] and Caffe2 [37]). In principle our system is general enough to be integrated into other ML frameworks.

For our initial system, we focus on the generation of CUDA code because NVIDIA GPUs dominate the hardware landscape for training deep neural networks. We believe our approach applies to other types of heterogeneous nodes with shared or partitioned memory.

The report comes with supplementary material labeled as Section A, covering background on polyhedral compilation and deep learning frameworks, implementation details and further experimental methodology.¹

2 Related Work

Despite decades of progress in optimizing and parallelizing compilation, programmers of computationally intensive applications complain about the poor performance of optimizing compilers, often missing the peak achievable performance by orders of magnitude. Among the reasons for this state of affairs, one may cite the complexity and dynamic behavior of modern processors, domain knowledge required to prove optimizations’ validity or profitability being unavailable to the compiler, program transformations whose profitability is difficult to assess, and the intrinsic difficulty of composing complex transformations, particularly in the case of computationally intensive loop nests [23, 25, 32, 15, 48, 4].

Several contributions have successfully addressed this issue, not by improving a general-purpose compiler, but through the design of application-specific program generators, a.k.a. active libraries [85]. Such generators often rely on feedback-directed optimization to select the best generation strategy

¹The report is meant to be easily accessible to a reader familiar with parallelizing compilation, performance tuning for GPUs, and a basic knowledge of the polyhedral framework, tensor algebra and convolution operations.

[77], as popularized by ATLAS [92] for dense matrix operations—and more recently BTO [9]—and FFTW [31] for the fast Fourier transform. Most of these generators use transformations previously proposed for traditional compilers, which fail to apply them for the aforementioned reasons. The SPIRAL project [69] made a quantum leap over these active libraries, operating on a domain-specific language (DSL) of digital signal processing formulas. Compilers for DSLs typically rely on domain-specific constructs to capture the intrinsic parallelism and locality of the application. Using such an approach, DSL compilers such as Halide [72] for image processing show impressive results. Its inputs are images defined on an infinite range, while TC sets a fixed size for each dimension using range inference. This is better suited to ML applications, which mostly compute on fixed size tensors with higher temporal locality than images; it is also less verbose in the case of reductions and does not carry the syntactic burden of pre-declaring stage names and free variables (Halide needs this as a DSL embedded in C++). OoLaLa [53] takes a similar approach for linear algebra, and TACO [46] and Simit [47] use a notation similar to that of TC, but generate sparse matrix code for numerical solvers.

Following this trend in the context of deep neural networks, we not only design yet another DSL and compiler but propose a more generic code generation and optimization framework bringing together decades of research in loop nest optimization and parallelization for high-performance computing. We also design the domain language to cover a variety of existing and emerging machine learning models. Our framework automates a combination of affine transformations involving hierarchical tiling, mapping, shifting, fusion, distribution, interchange, on either parametric or fully instantiated problems, that are not accessible to Halide [72, 57], Latte [82] or XLA’s [36] representations of tensor operations.

The polyhedral framework is a powerful abstraction for the analysis and transformation of loop nests, and a number of tools and libraries have been developed to realize its benefits [28, 12, 88, 11, 95], including components for production compilers such as GCC (Graphite) and LLVM (Polly). Polyhedral techniques have also been tailored for domain-specific purposes. State of the art examples include the PolyMage [59] DSL for image processing pipelines and the PENCIL approach to the construction of parallelizing and compilers for DSLs [3, 7]. Interestingly, some optimization techniques derived from PolyMage crossed over from polyhedral representations into Halide’s recent automatic scheduler [58]. Our compiler implements optimizations specific to the long, non-uniform reuse patterns and deeply nested loops of deep learning models; these heuristics are not available in Halide and variants [59, 57].

Back to deep learning frameworks, TC shares several motivations with Latte [82], including a high level domain-specific language and an end-to-end flow. TC provides an element-wise access that is just as expressive when implementing custom layers, but unlike Latte it is more concise thanks to type and shape inference, safer regarding static bound checking and graph connectivity, and more flexible by decoupling indexing from representation and layout choices (e.g., sparse layers). In addition, our framework implements more complex scheduling and mapping transformations than Latte, some of which are essential to GPU targets with partitioned memory architectures. Unlike Latte, it is also designed as a JIT compilation library for seamless integration with deep learning frameworks.

Like tensor comprehensions, XLA [36] provides automatic shape and size inference, it may operate “in process” as a JIT compilation library, and it integrates into a production deep learning framework (TensorFlow, Caffe2 [37]). XLA shares many motivations with Latte, with a focus on integration and completeness of functionality rather than on the complexity of the optimizations and mapping strategies. Most of our design and algorithmic contributions would naturally fit XLA, except for the following: TC remains independent from a specific computation graph framework while preserving tight integration with production frameworks; we did not use an embedded DSL approach—keeping C++ as an interface for implementing optimization strategies only—isolating the user from complexity and debugging hurdles of embedded DSLs.

Most recently, R-Stream-TF [67] was presented as a proof-of-concept adaptation of the R-Stream polyhedral compiler to the automatic optimization of TensorFlow operators. Similarly to our approach, the generated code is wrapped as a custom operator of TensorFlow. The tool takes a computation graph as input and partitions it into subgraphs amenable to tensor fusion, contraction and layout optimization. R-Stream-TF also leverages the broadcast semantics of TensorFlow to maximize the operator’s polymorphism w.r.t. input tensor dimension and shapes. This makes R-Stream-TF very aggressive in terms of static memory management and kernel partitioning. We made the

more pragmatic choice of leaving most of these decisions to the level of tensor algebra, allowing a domain-specific optimizer or ML expert to rewrite declarative comprehensions into capacity- and layout-optimized ones. On the contrary, TC is more ambitious in its domain-specialization of affine scheduling and mapping, aiming for the generation of a single accelerated kernel, with heuristics adapted to the high dimensionality and non-uniform, long reuse patterns of neural networks. The lack of algorithmic detail in the paper does not let us compare those affine transformation heuristics at the time of writing.

3 Tensor Comprehensions

We provide a language for expressing element-wise computations of tensors using *tensor comprehensions*.

Tensor Comprehensions (TC) are a notation for computing on multi-dimensional arrays that borrows from the Einstein notation (a.k.a. summation convention):

1. index variables are defined implicitly by using them in an expression and their range is inferred from what they index;
2. indices that appear on the right of an expression but not on the left are assumed to be reduction dimensions;
3. the evaluation order of points in the iteration space does not affect the output.

Let us consider matrix-vector product as a simple example of a tensor comprehension with two statements:

```
def mv(float(M,K) A, float(K) x) → (C) {
  C(i) = 0
  C(i) += A(i,k) * x(k)
}
```

This defines the function `mv` with `A` and `x` as input tensors and `C` as output. The statement introduces two index variables ‘`i`’ and ‘`k`’. Variables not defined anywhere, implicitly become index variables. Their range is inferred based on how they are used in indexing (see below); here we will discover `i = [0,M)`, and `k = [0,K)`. Because `k` only appears on the right-hand side, stores into `C` will *reduce* over `k` with the reduction operator `+`. Reductions can occur across multiple variables, but they all share the same kind of associative and commutative operator (e.g., `+=`) to ensure that evaluation order does not affect the computed value (e.g., composition of `min` and `max` do not commute, `min(max(f(.))) ≠ max(min(f(.)))`).

Intuitively, a tensor comprehension may be thought of as the *body* of a loop whose control flow is inferred from context. The equivalent C-style pseudo-code is:

```
tensor C({M}).zero(); // 0-filled single-dim tensor
parallel for (int i = 0; i < M; i++)
  reduction for (int k = 0; k < K; k++)
    C(i) += A(i,k) * x(k);
```

Importantly, the nesting order (`i` then `k`) is arbitrary: the semantics of a tensor comprehension is always invariant by loop permutation.

TC allows in-place updates, but preserves a functional semantics that is atomic on full tensors: the semantics is to *read RHS expressions in full before assigning any element on the LHS*. This specification is important in case the LHS tensor also occurs in RHS [30]: the compiler is responsible for checking the causality of in-place updates on element-wise dependences. We currently implement a simple syntactic check, allowing only in-place updates on pointwise definitions and tensor contractions. When this check fails, the compiler rejects the program due to liveness interference; for example, any in-place transposition `a(i,j) = a(j,i)` is incorrect (unless the range is empty or a single element), while `a(i,j) = b(j,i)` is a valid transposition. Of course, this explicit reuse and atomic update semantics does not preclude other scheduling and storage mapping decisions by the compiler, as long as these preserve the element-wise dependences of the TC. This mixed declarative-imperative design of TC is inspired from Lush [13].

```

def sgemm(float a, float b,
          float(N,M) A, float(M,K) B) → (C) {
  C(i,j) = b * C(i,j)      # initialization
  C(i,j) += a * A(i,k) * B(k,j)  # accumulation
}

```

Figure 1: Tensor Comprehension for the `sgemm` BLAS

Reductions in TC are often initialized with the reduction operator’s neutral element; we provide a short-cut for an *initializing reduction*, appending ‘!’ to the reduction symbol, i.e., ‘+=!’ instead of ‘+=’. Here is a one line definition of the matrix-vector product:

```

def mv(float(M,K) A, float(K) x) → (C) {
  C(i) +=! A(i,k) * x(k)
}

```

Using these simple properties, common machine learning kernels can be written in just a few lines. For instance, Figure 1 shows the SGEMM function of the BLAS library. General tensor contractions can be expressed along the same lines. A fully connected layer followed by a rectified linear unit takes the form of a transposed matrix multiplication initialized to a broadcast bias term and followed by pointwise clamping (i.e., `fmaxf` with 0):²

```

def fcrelu(float(B,I) in, float(O,I) weight,
           float(I) bias) → (out) {
  out(i,j) = bias(j)
  out(b,o) += in(b,i) * weight(o,i)
  out(i,j) = fmaxf(out(i,j), 0)
}

```

Here we chose to reuse the out tensor across all comprehensions, indicating the absence of temporary storage.

A 2-D convolution is similarly simple, its reduction is initialized to 0 (note the use of `+=!`):

```

def conv2d(float(B,IP,H,W) in,
           float(OP,IP,KH,KW) weight) → (out) {
  out(b,op,h,w) +=! in(b,ip, h + kh, w + kw)
                  * weight(op,ip,kh,kw)
}

```

with reduction dimensions `kh, kw`. A max pooling layer is:

```

def maxpool2x2(float(B,C,H,W) in) → (out) {
  out(b,c,i,j) max=! in(b,c, 2 * i + kw, 2 * j + kh)
  where kw in 0:2, kh in 0:2
}

```

In the case of max pooling, the indexes `kw` and `kh`, which determine how many entries to pool over, are under-constrained since they are not inferable from any input tensors and the range inference procedure emits an error when no further information is provided about these indices. So we provide a `where` annotation to inform the inference algorithm of the intended ranges of these variables and let it infer the remaining ranges from context.

Subscript expressions can be any affine function of iterators, or subscript-of-subscript expressions, and combinations thereof. The latter capture data-dependent accesses such as a gather operation:

```

def gather(float(N) X, int(A,B) I) → (Z) {
  Z(i,j) = X(I(i,j))
}

```

²For historical reasons related to the expression of element-wise linear algebra in the context of neural networks, the expression in matrix form often involves transpositions. TC lifts that impedance mismatch and makes it non-surprising: the tensor layout and sizes must match what is expected from the indexing expression.

TC closely matches an algorithmic notation. This is not true of today’s prominent frameworks where most operators are defined as black-box functions. The design of TC makes it easy to experiment with small layer variations, while preserving a concise, in-place expression. For instance, recently, strided convolutions have become popular in image classification [93]. With tensor comprehensions, a strided convolution is easily created as a tweak on convolution, here is a convolution strided by `sh` along `h` and `sw` along `w`:

```
def sconv2d(int sh, int sw, float(N,C,H,W) I,
           float(F,C,KH,KW) W, float(F) B) → (O) {
  O(n,f,h,w) = B(f)
  O(n,f,h,w) += I(n,c, sh * h + kh, sw * w + kw)
                * W(f,c,kh,kw)
}
```

Note that efficient implementations of `sconv2d` can take advantage of partial evaluation for the frequent case where `sh` and `sw` are constant, resulting in affine subscript expressions. This is another advantage of JIT compiling TC.

3.1 Range Inference

Tensor comprehensions are concise because most of the time loop ranges are inferred from context. Similar to the inference of polymorphic data types, the inference algorithm aims to accurately infer the range based on usage patterns. It is not always possible however, due to non-affine expressions or under-constrained problems—see e.g., max pooling. TC needs additional annotations for such cases.

Iteration variables are always non-negative. Unless specified otherwise in a `where` clause, each iteration variable is assumed to start at 0.

Inference is computed from input arguments to output tensors, setting up a constraint-based analysis problem across all the affine array accesses in a TC function. We initially looked for a very general setting of this problem, with an inference algorithm relying on Presburger arithmetic as implemented in polyhedral libraries [87]. Yet, to program productively, one must be able to mentally emulate the written code on the abstract machine defined by the language semantics. If this requires more thought than writing explicit loops would, our language design has failed. With this in mind, we eschew heavy-duty mathematical tools, and take a more straightforward approach for the sake of usability. We infer ranges only in cases where we feel they are obvious, and require explicit annotation elsewhere. We intend to fine-tune this boundary in the future depending on what users find surprising.

To find a good first approximation, we infer rectangular ranges that are as large as possible without reading out of bounds on the inputs. If there is more than one way to do this, we throw an error and require explicit annotation using a `where` clause.

This rule is sufficient to understand the `sgemm` case above. Maximizing the range of `i` gives it the range of the number of rows of `A`. Similarly maximizing the range of `j` gives it the range of the columns of `B`. `k` is used twice, so making `k` as large as possible gives it the lesser of the number of columns of `A` and the number of rows of `B`. These in turn are constrained to be equal by the type signature of the function (they are both `K`).

Now consider a simple 1-D convolution:

```
def conv1d(float(M) I, float(N) K) → (O) {
  O(i) = K(x) * I(i + x)
}
```

There are multiple ways in which we could maximize the ranges of `i` and `x`. If we first maximize `i`, we might say that it ranges over the entirety of `I`. This forces `x` to take on a single value only, which will not result in the output one expects from a convolution, as it ignores most of the kernel! If we first maximize `x`, so that it ranges over the entirety of `K`, then in order to not read out of bounds the range of `i` must be smaller, and we get an output that is slightly smaller than the input. This is the behavior we prefer.

In order to make this unambiguous without requiring explicit annotation in this simple case, range inference proceeds in rounds. We maintain a set of unresolved variables. Initially, this set contains all variables not constrained with an explicit `where` clause. In each round, we consider

all the tensor argument expressions that contain a single unresolved variable, and construct a boolean expression that states the access is not out-of-bounds. We then use tools from Halide (`solve_for_inner_interval`) to find the maximal range for the variable that satisfies this condition, given the ranges of variables already resolved in previous rounds. If the variable was already constrained in this round by some other tensor access, we take the intersection of the inferred ranges.

For the stencil above, in the first round we ignore the expression $I(i+x)$ because it contains multiple unresolved variables. We use the expression $K(x)$ to deduce a range for x . In the second round, $I(i+x)$ now contains a single unresolved variable, and we use the already-inferred range of x to deduce a maximal range for i . In other words, the access $K(x)$ constrains x to range from 0 to $N - 1$, while the access $I(i+x)$ constrains $i+x$ to range from 0 to $M - 1$, from which we deduce that i must satisfy the following constraint

$$\forall x \in [0, N - 1], i + x \in [0, M - 1],$$

which yields the final range of 0 to $M - N$ for i .

Notice the \forall universal quantification on i , constraining the output tensor O to be uniformly defined across the entire domain from the exact same inputs in I . This differs from the approach taken in the Alpha language for systems of affine recurrent equations [51] where the domain scanned by x would be the projection of the triangular domain of (i, x) involving existential quantification: $\{x \mid x \geq 0 \wedge \exists i \in [0, N - 1], i + x \in [0, M - 1]\} = [0, M - 1]$. The semantical choice of quantifying iterators universally is derived from Halide; it guarantees that the shape of input tensors is always a (hyper-)parallelepiped, it is intuitive to ML experts and facilitates the generation of compact code, free of conditional control flow—unlike a more conventional projection semantics.

More complex examples involve intersecting successive rounds of inference over the same variables, and also ambiguous cases where no single rectangular shape can be derived from a more general set of constraints. The latter will not type-check and the compiler will request the insertion of a disambiguating `where` clause.

In addition, since memory management is externalized to a ML framework, the list of temporary tensors defined within a TC must be made explicit—with their shape and ranges; the range inference algorithm infers this list automatically. Finally, the inference algorithm can be formalized as a type and effect system [61], collecting constraints on index sets along the sequence of tensor definitions.

In its first release, TC does not support recurrent definitions such as those needed for the implementation of Recurrent Neural Networks (RNN).

Note that tensor indexing may involve any integer-valued expression, as long as it does not depend on the LHS tensor of the current statement. The compiler does its best at range inference and in the static verification that individual elements are defined only once in an imperatively-defined dimension; compilation fails in case range inference does not succeed and no `where` clause is there to provide the missing information.

3.2 Data Layout Transformations

TC makes global data layout transformations significantly easier. The ML community has been heavily relying on such transformations by composing operations on tensor metadata in the form of a tuple of (`dataPtr`, `offset`, `size[]`, `stride[]`) [9]. One of the main usage ML researchers have for such primitives is algorithmic tiling and hierarchical decompositions. The former has strong connections to data tiling and is now ubiquitous in the implementation of high-performance convolutions in the frequency domain to keep the memory footprint under control [83] or to fit to fast local memories [2]. The *unfold* operation in Lush [13] and Torch [24] perfectly matches implicit data tiling (i.e., without explicit memory copies), when there are no partial border effects. TC supports generalized tensor transpositions (i.e., applying an n -D permutation matrix where $n > 2$) and data tiling can be achieved by simply reshaping tensors and adjusting the TC index expressions. Range inference and checking guarantees such reshaping will always be consistent throughout a TC. Array-of-struct to struct-of-array conversions—and similar operations on short vectors—are available by-products: they are particular cases of dimension interchange and data tiling. At this time, data layout and TC transformations are left to the domain expert at source level, the TC inference procedure guarantees the expressions have the proper ranges. We will reevaluate this assumption in the future as we introduce automatic data layout transformations in TC.

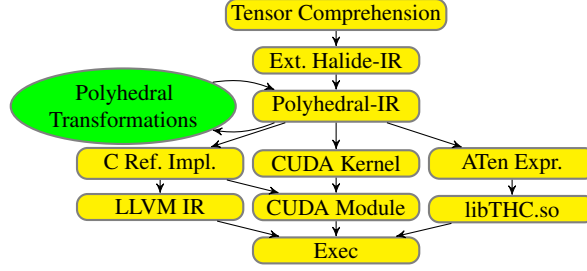


Figure 2: The JIT compilation flow lowers TC to Halide-IR, then to Polyhedral-IR, followed by optimization, code generation and execution

4 High-Level Workflow Description

Let us position our work in the context of deep learning frameworks such as TensorFlow, Caffe2 and PyTorch.³

TC expressions are first integrated into the ML framework as follows. We opted for an “in process” implementation, streamlining the interaction with computation graph engines and ML applications built on top of them, a unique feature for a fully-automated scheduling and mapping flow. We provide a thin API that translates the specific tensor object model to our own. Operator definitions are overridden to generate TC rather than the framework’s backend implementation, as well as provide users the ability to write their own TC.⁴ In this context, a single TC may correspond to a DAG of operators in the ML framework. This matching is currently done manually. Automatic DAG partitioning, matching and rewrites (like e.g., TensorRT [62]), informed by our compilation flow, are left for future work. The TCs are then JIT compiled as shown in Figure 2. In cases where the default backend implementation performs better, we fall back to the reference implementation.

Starting from a TC with specialized tensor sizes and strides,⁵ we lower it to a parametric Halide expression.

In a prototype version of the system, Halide-IR was lowered to polyhedral representation via a translation to PENCIL [3] and then parsed using the pet [89] and isl [86] libraries. To reduce the impedance mismatch between IRs and to facilitate the propagation of semantical annotations, the flow evolved to lower Halide-IR directly to a polyhedral representation, bypassing the PENCIL intermediate language.

Similarly, we bootstrapped CUDA kernel generation in the original prototype from a modified version of the PPCG compiler [88]. The modifications included its usage as a library, for in-process, multi-threaded operation (see Section 5). When moving away from PENCIL, the functions of PPCG were reimplemented from the ground up, aiming for more modularity and compliance with a modern C++ environment.

Complementing this flow, an autotuner and a serializable compilation tightly interact with scheduling and mapping strategies to search the transformation space (see Section 6).

Additionally, we provide a simple “identity” polyhedral mapping option to generate a naive, readable, CUDA reference implementation that may be run and checked for correctness on a single GPU thread and shake off simple problems. We are planning a simple LLVM JIT compilation pass to make that reference implementation more generally usable on a CPU, but this is not yet implemented.

Lastly, we will provide a path to emit a series of library calls, a useful fallback to default implementations backed by CUDNN.

³See Section A.1 for a brief introduction to these frameworks.

⁴Section A.2 describes the programming interface for TC.

⁵Our toolchain supports parametric specifications, yet we have found early specialization to be beneficial in driving profitability decisions during polyhedral scheduling.

5 Polyhedral JIT Compilation

The compiler bridges the impedance mismatch between the logical layout of high level tensor operations (dimension ordering) and the data format the polyhedral code generator expects (C99 arrays [3]). The lowering step ensures combinations of size and stride correspond to non-aliasing array and subarray syntax; it also ensures the absence of out-of-bounds access, analyzing access relations and inferred tensor ranges; it emits tensor declarations and reorder expressions to match the data model of the target language, i.e., row-major arrays.

Note that tensor specifications may feature input and output arguments aliasing for in-place computation and implicit conversion of tensors of higher dimension. We argue that such specifications should lead to multi-versioning and specialization for each aliasing scenario. Also, the semantics adopted by TC, building on range inference, differs from NumPy-style “broadcast” semantics adopted in some form or another by XLA, PyTorch and MXNet.⁶ TC does not need such implicit syntactic sugar. For example, the TC corresponding to the so-called outer product matrix multiplication $[p, q, r] \text{ matmul } [1, s, r, t] \rightarrow [p, s, q, t]$ is simply:

```
def outerProductMM(float(P,Q,R) A, float(S,R,T) B) → (O) {
  0(p,s,q,t) +=! A(p,q,r) * B(s,r,t)
}
```

One may further transform layouts and derive a QPTS version (named by the ordering of output dimensions) instead of PSQT if desirable.

Additional lowering steps include forward substitution of convolution expressions (storage/computation tradeoff), padding with zero, mirroring and clipping.

The *polyhedral framework* offers a state-of-the-art internal compiler representation of loop-based programs that are “mostly regular” [29]. In its most basic form, it describes arithmetic expressions surrounded by loops and branches whose control flow can be determined statically. Hence the polyhedral framework is said to operate on *static control parts* (SCoP) of the program. More specifically, loop bounds and branch conditions are affine expressions of outer loop iterators and statically unknown constant values that are treated symbolically and referred to as *parameters*. Computation is described using arithmetic expressions on array elements with the same restrictions on subscripts as on loop bounds. Extensions exist to handle irregularities through over-approximation [10] or user-defined annotations [3]. Despite its deceiving apparent simplicity, the framework captures large classes of computation-intensive codes, it is parametric on domain and array sizes, and more expressive than domain-specific representations such as Halide’s.

This work demonstrates that the polyhedral framework is particularly well suited for deep neural networks, associated with large and deeply nested loops with long dependence chains and non-uniform or all-to-all patterns—arising from fully connected layers and tensor contractions and transpositions. These features push the optimization problem into a different heuristic space than Halide’s for image processing, and a much wider space than linear algebra alone.

We use the *named relation notation* introduced in `iscc` [87] for unions of relations where tuples of iterators are guarded with syntactic identifiers [68]. The reader unfamiliar with polyhedral compilation—iteration domains, affine access and dependence relations, scheduling and polyhedral code generation—may refer to Section A.3 in the supplementary material.

Schedule Trees Affine maps can be composed into *schedule trees* [90] to facilitate the communication of properties from the high-level language (here, TC) to the downstream optimizer and to attach target-specific information along the way (e.g., SPMD thread-relative induction as in CUDA, synchronization, data transfer instructions [88, 3]). Schedule trees introduce specific node types. A *band node* defines a *partial* execution order through one or multiple piecewise affine functions defined over iteration domains. The name refers to the notion of a *permutable schedule band*, a tuple of one-dimensional schedule functions that can be freely interchanged while preserving the semantics of the program. An affine function in a band is often referred to as a *band member* or a *schedule*

⁶Broadcasting is a set of non-trivial rules that allow implicit conversion between tensors of different dimensions. It enables certain tensor operations even when an appropriate library implementation does not exist for those non-conforming shapes. It carries its baggage and ambiguities when dealing with higher dimensional tensor contractions, as demonstrated in the TensorFlow Github issue #5523.

dimension. A collection of *filter nodes* partitions the iteration space, binding its subtree to a subset of the iteration domain. They can be arranged into *set* or *sequence nodes* depending on whether the order of execution must be constrained for correctness or not (i.e., whether or not it corresponds to an `#pragma omp sections`). *Context nodes* provide additional information on the variables and parameters, e.g., tensor extents or GPU grid/block sizes; they may also introduce local scopes and parameters constant within a subtree, which is useful when mapping induction variables to block and thread identifiers in CUDA. Finally, *extension nodes* introduce auxiliary computations that are not part of the original iteration domain, which is useful for, e.g., introducing statements copying data to and from shared memory.

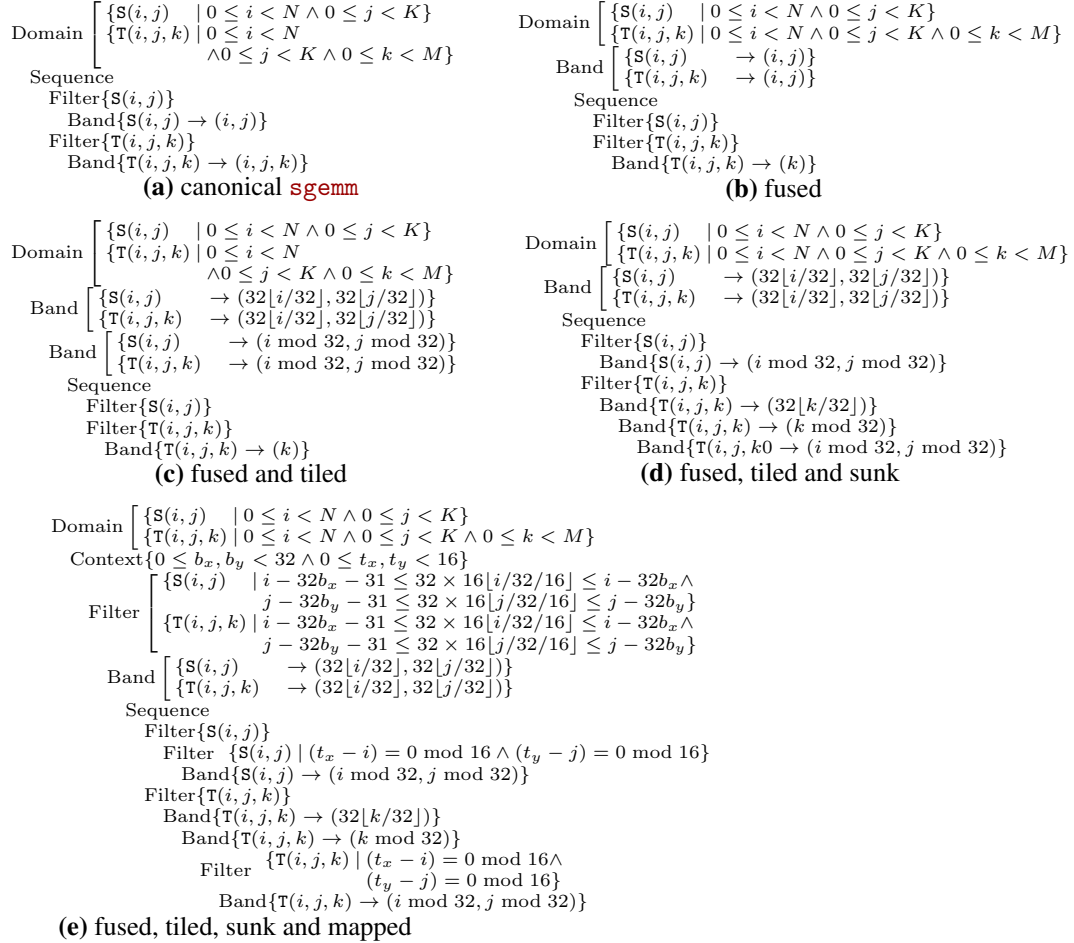


Figure 3: Optimization steps for **sgemm** from Figure 1

A *canonical* schedule tree for a TC is defined by an outer Sequence node, followed by Filter nodes for each TC statement. Inside each filtered branch, Band nodes define an identity schedule with as many one-dimensional schedule functions as loop iterators for the statement. Implicit loops form a permutable band as per TC semantics. Figure 3.a shows the canonical schedule tree for the **sgemm** TC—declaration of parameters $(N, M, K) \rightarrow \{\dots\}$ is omitted hereinafter for brevity.

One recognizes a 2-D nest for the initialization statement followed by a 3-D nest for the update statement. The schedule can be either parametric in input sizes, or have extra context information on the tensor sizes. In cases where Band nodes do not define an injective schedule, the statement instances are scheduled following the lexicographical order of their domain coordinates. Program transformation in the polyhedral model involves defining a different schedule, which corresponds to a different (partial or total) order of traversing the iteration domain. For example, observing that the C tensor is reused between two nests, one can construct the schedule in Figure 3.b to leverage access locality and improve performance. This tree features an outer band node with i and j loops that became common to both statements, which corresponds to *loop fusion*. The sequence node ensures

that instances of S are executed before respective instances of T enabling proper initialization. The second band is only applicable to T and corresponds to the innermost (reduction) loop k . Additionally, the tree introduces a Context node to state the assumptions about the values of parameters.

Out-of-bounds accesses The polyhedral model allows for relational encoding of tensor accesses. Composing those with the iteration domains expressed as sets allows for computing the set of all accessed tensor elements, i.e., the statement’s footprint, and for checking whether it fits the (specified or inferred) tensor sizes. In particular, access relations enable the detection of out-of-bounds accesses. Elements that belong to the footprint $\mathcal{F} = \mathcal{D}.\mathcal{A}$, but not to the set of tensor elements \mathcal{T} , inferred from the tensor shapes, correspond to out-of-bounds accesses. Hence, $(\mathcal{D}.\mathcal{A}) \setminus \mathcal{T} = \emptyset$ is a condition for the absence of out-of-bounds accesses.

5.1 Polyhedral Transformation and Mapping

When targeting a parallel architecture, program transformations involve a change of schedule and also a mapping strategy; these must respect the dependences while optimizing for target-specific properties. Beyond guaranteeing the validity of the transformation, dependences can be used to expose parallelism (independent instances can be executed in parallel) or to improve data access locality (dependent instances executed close in time). Several efficient scheduling algorithms exist, focusing on a combination of parallelism, locality and vectorization [91, 12, 95, 84, 65]. Our transformation engine is based on four components:

1. core polyhedral scheduling is provided by *isl*, which automatically optimizes for (outer) loop parallelism and locality; we tuned the affine scheduling heuristic towards folding a complete TC program into a single GPU kernel;
2. the schedule is further tiled to facilitate the mapping and temporal reuse on the deep parallelism and memory hierarchy of GPUs [91];
3. mapping to GPUs borrows from algorithms previously implemented in PPCG [88], with additional extensions to support the more complex and imperfectly nested structures appearing in ML kernels;
4. memory promotion deals with explicit data transfers to and from shared and private memory spaces. These components and the TC-specific extensions are detailed below.

5.2 Scheduling

The core part of the *isl* scheduler iteratively solves integer linear programming problems to compute piece-wise affine functions that form schedule bands. It also ensures that these bands are permutable and can be further tiled. Internally, it builds a data dependence graph (DDG) where nodes correspond to statements and edges express dependences between them. Each edge is annotated with a set of “typed” dependence relations. The *isl* scheduler [91] is designed for better scalability since integer linear programming has exponential complexity in the worst case. In particular, it introduces the *affine clustering* technique that is based on computing the schedule bands separately for individual strongly-connected components of the DDG and then clustering these components iteratively and scheduling with respect to each other. Clustering not only decreases the size of the linear problems the scheduler has to solve, but also serves as a basis for *isl*’s loop fusion heuristic.

We extended the *isl* scheduler to provide the caller with a more fine-grained control over the scheduling process. For affine transformations, the user can supply additional arbitrary constraints to be inserted in the linear program. For clustering, the user can supply a decision function for pairwise dependence graph component combination, after it was demonstrated to be valid by the scheduler. These configuration points serve as a basis for *scheduling strategies*. With these strategies, affine transformations can be restricted to: (1) non-negative schedule coefficients and/or, (2) non-skewing transformations (i.e., loop interchange and shifting). Clustering decisions allow for control over the conventional minimum and maximum fusion targets, and additionally, maximum fusion that preserves at least three nested parallel loops (to be mapped to CUDA blocks and threads). Scheduling strategies can be configured and selected through the autotuning process. In all cases, we enforce that a single GPU kernel is generated.

5.3 Imperfectly Nested Loop Tiling

Loop tiling is implemented as a separate step after the scheduling took place and performed as a schedule tree transformation. Essentially, it converts a permutable schedule band into a chain of two bands with the outer band containing tile loops and the inner band containing point loops with fixed trip count. This can be seen as a conventional strip-mine and sink transformation. For example, Figure 3.c shows the schedule tree for the fused and tiled `sgemm`.

In addition to conventional loop nest tiling, the schedule tree representation allows a tiling of imperfectly nested loops. The technique is based on the following observation: if a loop does not carry dependences (i.e., is parallel), it can be sunk below any other loop. In valid schedules, all dependences are carried (or satisfied) by some loop, along which they feature a positive distance. A dependence is only violated if it has a negative distance along some loop *before* it is carried by another loop [45]. Parallel loops do not carry dependences by definition and therefore do not affect dependence satisfaction or violation. Therefore, imperfectly nested tiling is implemented by first tiling all bands in isolation and then sinking parallel point loops in the tree. During this process, the point band is replicated in each subtree below a sequence (or set) node and its schedule is updated so that it only contains relevant domain points.

The schedule tree for `sgemm` purposefully has two imperfectly nested bands. Dependence analysis shows that loops `i` and `j` are parallel. Therefore, we can tile them and sink the point loops below the band of the reduction `k` loop, resulting in the schedule tree in Figure 3.d. Innermost nested bands with point loops can be joined together into a single band after checking for permutability.

5.4 Mapping to Blocks and Threads

A schedule tree can also be used to represent the *mapping* to an accelerator, in particular a GPU with multiple blocks and threads. This operation is performed by associating certain schedule band members, and the corresponding loops, to thread or block indexes. Polyhedral code generator then omits the loops, if possible, and rewrites the index expressions accordingly. Our mapping algorithm is derived from the one originally designed for PPCG, where grid and block sizes are specified independently from tile sizes. Due to the semantics of blocks and threads, only parallel loops that belong to a permutable schedule band can be mapped. If point loops are mapped to threads, the ratio between tile sizes and blocks sizes controls the number of iterations executed by each thread. Note that tile sizes smaller than the block sizes lead to some threads not performing any computation, if it is the point loops of the tiling that end up getting mapped to threads.

We require the schedule tree to have at least an outermost band with outer parallel dimensions. Contrary to PPCG, which maps each of possibly multiple outer bands to both blocks and threads (after tiling), our mapping algorithm maps a single band to blocks in order to generate a single kernel as expected by ML frameworks, while multiple bands can be mapped to threads. The parallel dimensions of the (single) outermost band are mapped to GPU blocks. In each schedule tree branch, the innermost permutable band, typically consisting of point loops, is mapped to GPU threads with the following restrictions. The number of mapped dimensions must be equal across branches. This may require mapping some thread dimensions to zero in some branches.

The mapping itself is performed by inserting special names, communicated to the code generator through a context node, and by associating them to band dimensions in filter nodes. For the matrix multiplication example, our mapping strategy produces the schedule tree in Figure 3.e. We introduced a context node in the schedule tree to indicate the effective sizes of the parameters as well as the grid and block sizes (denoted as b_x, b_y and t_x, t_y , respectively, standing for values potentially taken by `blockIdx.xy` and `threadIdx.xy`). This insertion is performed just-in-time, when the effective tensor sizes are known. Also pay attention to the Filter nodes referring to b_x, b_y, t_x and t_y parameters. These nodes express the *mapping* to the GPU.

5.5 Memory Promotion

We are interested in promoting parts of tensors into shared or private GPU memory. While the promotion decision is taken by a heuristic and the corresponding imperative code is generated at a later stage, schedule trees offer a convenient interface for attaching memory-related information. Memory promotion is based on the notion of *array tile*, a form of data tiling for software-controlled

local memories. It is a constant-size potentially strided block in the array that covers all elements accessed within a given (schedule) tile. We revisit and extend PPCG’s support for memory promotion [88, 91].

Promotion of Indirectly Accessed Arrays. Our memory promotion approach also handles indirectly accessed arrays. Without loss of generality, consider the access $O[1 + \text{Idx}[i][j]][k]$. We refer to O as outer array and to Idx as index array. In case of nested indirections, outer/index pairs are processed iteratively from innermost to outermost. While the values taken by the first index expression of the outer array are unknown statically, we can still cache them locally as $\text{shared_O}[1][i][j][k] = O[1 + \text{Idx}[i][j]][k]$. Because some values can be duplicated, indirect promotion is only possible if both the outer and the index arrays are only read, writing to them could result in different values that cannot be trivially merged. In general, we require the index array to have an array tile, i.e., only a fixed-sized block of it is accessed. When computing the array tile for the outer array, we ignore the indirect parts of the subscript (affine parts are treated as usual). We then introduce as many additional index expressions in the promoted outer array as there are in the index array. Extents of the array along these new dimensions correspond exactly to the array tile sizes of the index array. Hence an element of the promoted array contains a copy of the global array element that would be accessed with the given index array. Indirect subscripts are only used when copying from the global memory while all other accesses are rewritten in the code generation. In presence of multiple indirect index expressions that share subexpressions and have equal tile sizes along the corresponding dimensions, it is sufficient to introduce a single index expression in the promoted array for all identical subexpressions.

Promotion Heuristics. Directly accessed arrays are promoted to shared memory if there exists an array tile of fixed size, if individual elements are accessed more than once and if at least one of the accesses does not feature memory coalescing. The latter is visible from the access relation with the schedule applied to the domain: the last access dimension should be aligned with the schedule dimension mapped to x threads. For indirect arrays, the coalescing requirement is dropped because of the presence of additional long memory dependences that these cases entail. The total amount of shared memory being fixed, we apply a simple greedy heuristic and refuse promotion if the required amount of shared memory would overgrow the available amount.

5.6 Mapping to Registers

There are currently no plans to implement more complex register promotion strategies than those previously supported by PPCG. This is a temporary, pragmatic choice, based on the following observations:

- except in limited cases [69, 80], we have not seen empirical evidence that automatically generating low-level code from a high-level specification results in a significant performance gain over assembly; additionally modern assembly generators are now publicly available and re-targetable [26];
- generalizing and re-targeting register optimization passes to different architectures with multiple vector lengths, alignment constraints and patterns is no easy task;
- many different strategies exist which include (1) pipelining at the register level, (2) register rotation, (3) multi-buffering, (4) new ISAs with collective-style semantics [63], some of which are not even available without significant genuflections;⁷
- often such strategies are first implemented with intrinsics and assembly as a proof of concept and can be easily templated and reused with a tool like PeachPy [26].

Performance results are slightly impacted by this temporary status of the implementation. We also plan to rely on external library calls, e.g., for accelerating reductions.

⁷E.g., the mix of register banking, $L - 1$ FPU operand reuse, and control code on Maxwell GPUs, reverse-engineered and exploited in MaxAS (<https://github.com/NervanaSystems/maxas>).

6 Autotuning and Caching

While polyhedral scheduling and mapping to GPUs is very cheap compared to training a neural network, it is far from usable in a traditional JIT setting. We take advantage of the mostly static structure of neural networks to cache and reuse the best results of the autotuned compilation pass of an operation/kernel under similar conditions (input shapes, target architecture, and optimization options). We exploit this reuse with a compilation cache.⁸

6.1 Compilation Cache

The compilation cache stores the generated CUDA or PTX code for a given TC. The generated code depends on the input shapes, the selected optimization options (e.g., tile sizes, loop fusion scheduling strategy, mapping decisions) and the constraints induced by the target GPU architecture (e.g., shared memory/register size, fraction of shared memory to use for occupancy purposes, etc...). Each cache entry key is therefore a tuple:

(TC, input, shapes, target, architecture) .

For the purpose of caching we use a summarily templated version of TC to make the key agnostic to name changes. Each cache entry holds the fastest known version. Before each kernel optimization the cache can be queried. On a cache miss, the regular JIT compilation flow is invoked. The cache is serialized to a protocol buffer interchange format [35] to enable persistence and reuse. To avoid long and unpredictable compilation and autotuning times, one may pre-populate the cache with reference implementations. Since the cache serializes to strings, we added the capability to inject entries into the cache to support particular cases of interest where low-level manual tuning helps (the experiments in the report do not make use of this). In the current implementation, the size of the compilation cache could potentially become cause for concern: for every operation, the number of input shapes and optimization options can be arbitrarily large. In practice, however, the number of operations of interest is limited (e.g., the total number of different operators in Caffe2 v0.8.0 is approximately 400) and the space of input shapes is very sparse. Further characterization of these statistics will be the subject of future work. Importantly, note that our whole pipeline is parametric and specialization can be injected at any point (or not injected at all). For the time being we choose to inject runtime sizes as early as possible in the polyhedral compilation flow (i.e., before polyhedral scheduling) because it eagerly propagates valuable information for scheduling, tiling, mapping and total elimination of non-loop control flow (in static cases). One good candidate for parametrization is the minibatch dimension. The minibatch dimension is usually mapped to CUDA grid dimensions. These grid dimensions are specified by the kernel launch call and can be changed without the need to generate a different version. A separate database which includes performance data for all versions is also maintained for use in autotuning. This will be useful when additional search techniques are implemented such as Bayesian hyperparameter search [78], multi-armed bandit optimization [64] or black-box optimization [34].

6.2 Autotuning

The autotuner interacts with the rest of the environment through the compilation cache, storing the best versions for later use. It includes the following steps, setting up:

1. a set of starting configurations that worked well for similar TCs, and a few predefined strategies for reference problems;
2. the tuning space dimensions and admissible values for ranges;
3. the type of search—currently a genetic algorithm or random.

The autotuner runs for a prescribed amount of time, updating the cache with better versions along the way. It uses genetic search [33] which operates on generations of candidate configurations. In each tuning step the candidates are compiled and profiled, then assigned a fitness value inversely

⁸Note that in a traditional dynamic setting such as stack-RNNs, few parameters vary and it is not unreasonable to compile multiple versions; we can also relax any dimension to remain parametric (the polyhedral framework handles parametric control-flow).

proportional to their runtime. Each new candidate is bred through three parent uniform cross-over and also undergoes mutation with a low probability.

1. three parents are selected probabilistically based on their fitness, the higher the fitness the higher the selection chance;
2. each “gene”, which corresponds to one tuning parameter, of the new candidate is randomly selected from the parents.

Every new candidate also undergoes mutation: there is a low probability that zero or more of its genes are assigned random values. This probability is called the mutation rate and it controls the exploration versus exploitation tradeoff.

Autotuning evaluates 100s to 1000s versions for each kernel. Search strategies such as genetic algorithms require evaluating multiple candidates before each search step; we take advantage of this property by launching multiple compilation jobs in parallel with our generic multi-threaded, multi-GPU autotuner (see Figure 4). The search strategy enqueues multiple candidate configurations in the “Compilation Jobs” queue; the candidate configurations are compiled in parallel by multiple CPU threads. Whenever a compilation job is finished the result is enqueued in the ‘Profiling Jobs’ queue; each profiling job is evaluated on an available GPU; the profiling results are used to update the autotuning database and to generate the next set of candidates.

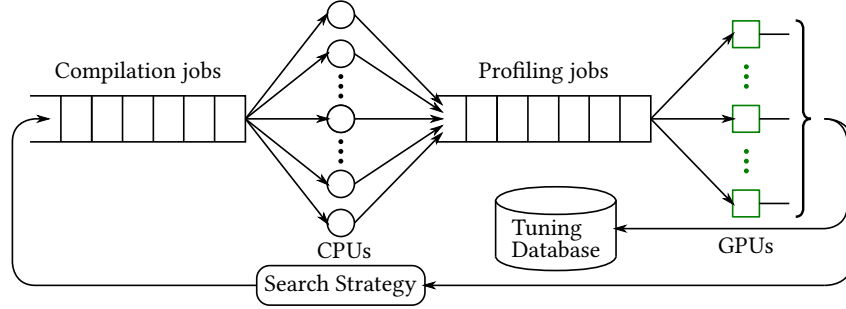


Figure 4: Multithreaded autotuning pipeline for kernels

A variety of kernel options are tuned:

- the search for tile, block, and grid sizes is narrowed to choices that help avoid tail effects; we consider both powers of 2 and integer ceil divisors of the problem sizes;⁹
- the bound on how many iterations can be unrolled on the bottom up paths from leaves to the root of the schedule tree; we consider powers of 2 up to 4096;
- discrete choices on fusion strategies and shapes of the admissible schedules, e.g., to prevent loop skewing and trade parallelism for locality;
- lower-level options such as shared or private memory usage and how aggressively to use those memory spaces in each block, which directly impacts GPU occupancy.

7 Examples And Performance Results

This section reports on the evaluation conducted on an earlier version used for a submission to the PLDI 2018 conference, relying on a modified version of the PPCG compiler [88]. The implementation and dependent packages in the public release of TC differ slightly, bypassing PENCIL [3] and reimplementing the necessary functions of PPCG.

We consider two systems for all experiments:

⁹Indeed, it is common to see problem sizes close to a power of 2 (e.g., 130) for which it is often better to avoid launching an extra block at the cost of a slightly off tile or mapping size (e.g., 65); this brings up to 30% benefits on latency-bound kernels.

- 8 Maxwell nodes with 2 socket, 12 core Intel(R) Xeon(R) CPU E5-2680 v3 @ 2.50GHz, with 8 Tesla M40 GPUs and 12GB of memory each;
- 8 Pascal nodes with 2 socket, 14 core Intel(R) Xeon(R) CPU E5-2680 v4 @ 2.40GHz, with 8 Tesla P100-SXM2 GPUs and 16GB of memory each.

We use CUDA v8.0, CUBLAS v8.0.45, CUDNN v6.0.21, NVRTC v8.0. Note that with NVRTC v8.0 we experience an extra overhead of around $15\mu s$ that can become more important than the kernel itself; this is understood to be reduced in NVRTC v9.0 [40]. When relevant, we discuss individual kernel performance measured with nvprof but *always report all our numbers with the full CPU overhead*, which includes a call to `cudaDeviceSynchronize`.

We report our baseline and best autotuned variant for every benchmark, together with the corresponding Caffe2 and ATen reference, when available.¹⁰ Note that Caffe2 is considered as one of the fastest ML frameworks.

The outputs are checked against the reference implementation. All benchmarks we report are run 1,000 times on the GPU. We report p0 (a.k.a. min), p50 (a.k.a. median) and p90 (90th percentile). The best autotuning results are serialized and saved in the compilation cache on disk. A subsequent validation procedure traverses the compilation cache for each example, selects the best mapping options and runs 1,000 iterations, checks against the reference implementation and logs the result. We autotune with 16 CPU threads and 8 GPUs per node. One full sweep of the genetic autotuner involves a population size of 100 over 25 generations and takes about 6 hours to complete. We find the bottleneck is often NVRTC compilation, in particular, we realized it acquires a global lock internally and can only process one kernel at a time.

Baseline mapping options are picked as “reasonable guesses”: we did not spend time performing manual tuning but did not choose a trivially bad solution either.¹¹ In particular, no iterative, user-involved, transform-inspect-evaluate loop is required and the polyhedral mapper already automates all decisions and also offers many different knobs that the autotuner can latch on. This should come as no surprise given the rich, 30-year history of the field of polyhedral compilation. We start our discussion with common kernels that are ubiquitous in ML workloads. We then show how TC fully automates the synthesis of CUDA kernels for research layers that do not yet have an existing HPC implementation. We conclude with a discussion of a model used in production.

Finally, in the context of ever increasing hardware computation capabilities, models that are bandwidth-bound today will increasingly shift towards the latency-bound regime. Specialization of kernel mapping close to that boundary crossing towards low-latency regimes is obtained automatically in this contribution.

We provide the baseline and best autotuner options in the supplementary material, and the final generated code where informative.

Transposed Matrix Multiplication In the context of deep learning, transposed matrix multiplication is ubiquitous:

```
def tmm(float(M,K) A, float(N,K) B) → (C) {
  C(m,n) +=! A(m,kk) * B(n,kk)
}
```

At the largest problem sizes, our best autotuned version is $4.2\times$ (resp. $3.4\times$ on Pascal) *slower* than Caffe2 with CUBLAS. The reader should note this hints at the improvement potential of TC, although:

1. this is one of the most hand-tuned kernel in history and CUBLAS operates close to peak at large enough sizes;
2. we do not implement register tiling and advanced promotion schemes for now (see Section 5.6) hence performance is bound by shared memory bandwidth;

¹⁰ATen—the asynchronous tensor library—currently wraps the Torch tensor library and is integrated with PyTorch. The ATen reference implementation is accessible from C++ and acts as a reasonable proxy for the expected PyTorch performance; but still not an apples-to-apples comparison.

¹¹It would be interesting to compare with Halide’s autoscheduler. Unfortunately, it is not currently functional for GPUs.

Common and Research Kernels

(B, M, K, N)		$(\text{nil}, 128, 32, 256)$			$(\text{nil}, 128, 1024, 1024)$			$(\text{nil}, 128, 4096, 16384)$			$(500, 72, 26, 26)$		
		p0	p50	p90	p0	p50	p90	p0	p50	p90	p0	p50	p90
tmm	Caffe2 + CUBLAS	33	35	36	127	134	136	3,527	3,578	3,666	340	347	350
	ATen + CUBLAS	35	35	36	120	123	125	3,457	3,574	3,705	342	348	353
	TC (manual)	32	33	35	441	446	469	24,452	24,583	24,656	166	170	172
	TC (autotuned)	28	29	30	309	313	316	14,701	14,750	14,768	96	101	110
tmm	Caffe2 + CUBLAS	29	30	31	107	108	109	2,404	2,431	3,068	189	192	197
	ATen + CUBLAS	26	27	27	104	106	108	2,395	2,409	3,043	188	190	191
	TC (manual)	21	22	23	188	194	210	8,378	8,402	8,411	91	92	93
	TC (autotuned)	24	25	26	107	110	111	8,130	8,177	8,251	51	53	54
(N, G, F, C, W, H)		$(32, 32, 16, 16, 14, 14)$			$(32, 32, 32, 32, 7, 7)$			$(32, 32, 4, 4, 56, 56)$			$(32, 32, 8, 8, 28, 28)$		
		p0	p50	p90	p0	p50	p90	p0	p50	p90	p0	p50	p90
gconv	Caffe2 + CUDNN	1,672	1,734	1,764	1,687	1,777	1,802	4,078	4,179	4,206	3,000	3,051	3,075
	ATen	N/A	N/A	N/A	N/A	N/A	N/A	N/A	N/A	N/A	N/A	N/A	N/A
	TC (manual)	6,690	6,752	6,805	3,759	3,789	3,805	2,866	2,930	2,959	3,939	4,009	4,045
	TC (autotuned)	666	670	673	1,212	1,215	1,216	1,125	1,144	1,159	847	863	870
gconv	Caffe2 + CUDNN	1,308	1,343	1,388	1,316	1,338	1,350	4,073	4,106	4,119	1,993	2,021	2,036
	ATen	N/A	N/A	N/A	N/A	N/A	N/A	N/A	N/A	N/A	N/A	N/A	N/A
	TC (manual)	3,316	3,339	3,345	2,327	2,348	2,363	1,683	1,691	1,694	1,845	1,870	1,883
	TC (autotuned)	319	321	322	691	705	714	464	481	504	371	377	379

Figure 5: Wall-clock execution of kernels (in μs). Each kernel ran 1000 times. The top half of each table is Tesla M40 (Maxwell) and the bottom half is Tesla P100 (Pascal); N/A indicates the framework lacked an implementation

Production Models

	1LUT			2LUT					
	p0	p50	p90	p0	p50	p90			
Caffe2 + CUBLAS	78	80	82	188	193	207			
ATen + CUBLAS	N/A	N/A	N/A	N/A	N/A	N/A			
TC (manual)	38	39	40	47	49	52			
TC (autotuned)	38	39	40	47	49	52			
Caffe2 + CUBLAS	63	64	66	122	125	128			
ATen + CUBLAS	N/A	N/A	N/A	N/A	N/A	N/A			
TC (manual)	21	22	23	30	31	32			
TC (autotuned)	21	22	23	30	30	31			
	MLP1			C3			MLP3		
	p0	p50	p90	p0	p50	p90	p0	p50	p90
Caffe2 + CUBLAS	123	125	135	146	159	164	124	128	142
ATen + CUBLAS	109	110	112	128	142	148	188	192	213
TC (manual)	150	157	159	344	349	351	67	68	70
TC (autotuned)	123	125	131	219	224	227	56	57	59
Caffe2 + CUBLAS	123	133	134	107	113	115	129	131	133
ATen + CUBLAS	98	98	99	105	110	112	164	167	168
TC (manual)	91	92	93	275	279	281	48	48	49
TC (autotuned)	79	80	80	117	128	129	45	46	46

Figure 6: Wall-clock execution of kernels (in μs). Each kernel ran 1000 times. The top half of each table is Tesla M40 (Maxwell) and the bottom half is Tesla P100 (Pascal); N/A indicates the framework lacked an implementation

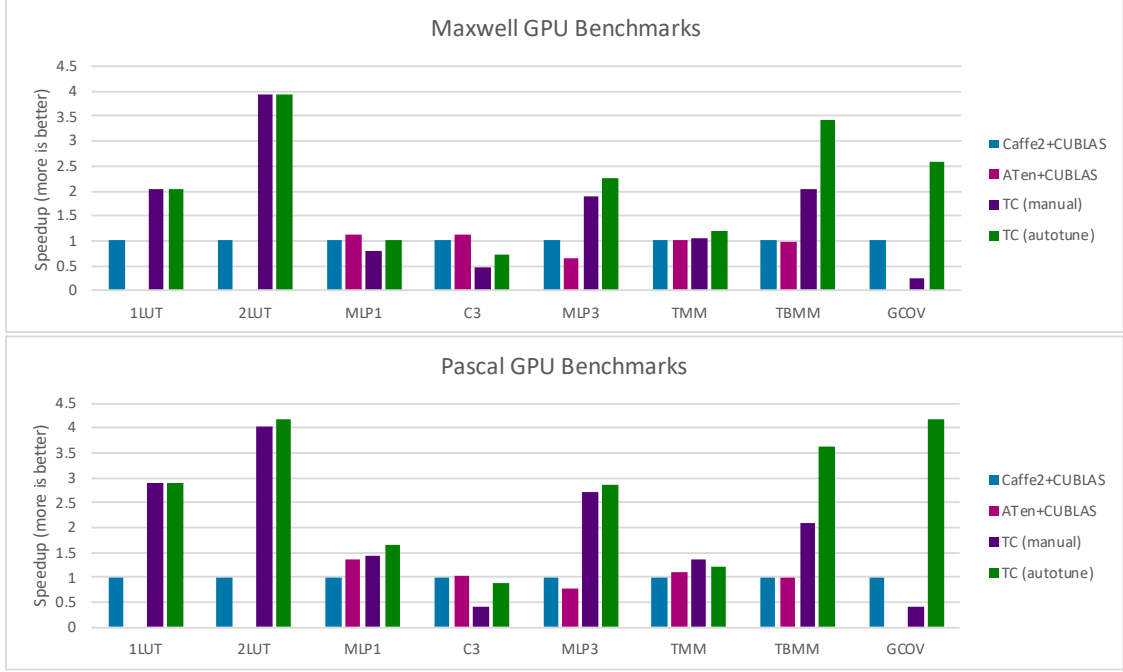


Figure 7: Speedup of the p50 (median) run time across configurations and benchmarks, for the smallest data sets, normalized to Caffe2-CUBLAS

- the amount of trickery required to extract the highest levels of performance has been documented by Scott Gray [38]. This involves FU operand reuse and SASS code generation to get past register bank conflicts. This is not accessible at the CUDA or even PTX levels.

On the up side:

- our kernel performs close to the peak shared memory bandwidth of the machine, it is as good as one can hope for in the context of Section 5.6;
- it exhibits non-trivial gains in the latency-bound regime;
- register tiling and reuse schemes are mundane in the polyhedral literature and could be implemented in the future;
- we believe a matching scheme for a library of optimized primitives is the most sensible, portable direction, as evidenced by Spiral [69], Spampinato et al. [79] and the NVIDIA Volta Tensor Cores [63]; this is work in progress;
- lastly, our TC abstractions make it very easy to call ATen and CUBLAS instead of our generated kernel, providing the user with strong guarantees performance will not be degraded.

Note that on smaller tensors, a.k.a. low-latency mode ($28\mu s$ on CPU), on Maxwell nvprof shows our best kernel takes $4.6\mu s$ while CUBLAS implements a dedicated kernel (`maxwell_sgemm_128x64_raggedMn_tn`) which takes $15.9\mu s$.

Transposed Batched Matrix Multiplication This is another common operation in which batches of matrix pairs are multiplied. Consider X and Y with dimensions (B, N, M) and (B, M, K) respectively, the corresponding TC is:

```
def tbmm(float(B,N,M) X, float(B,K,M) Y) → (Z) {
  Z(b,n,k) +=! X(b,n,m) * Y(b,k,m)
}
```

For sizes relevant to Factorization Machines [75], $(B, N, M, K) = (500, 26, 72, 26)$, the *speedup* reaches $3.5\times$ (resp. $3.7\times$ on Pascal) over CUBLAS—nvprof reports $78\mu s$ vs. $325\mu s$ for the dedicated kernel (`maxwell_sgemmBatched_128x128_raggedMn_nn`).

Grouped Convolutions Grouped convolutions have been present for a few years in the DNN research community, they were already used in the Dropout [42] network and have recently gained traction as part of the state-of-the-art ResNext [93] model.¹² Compared to a traditional 2-D convolution, a grouped convolution takes the large reduction on the input channel dimension and splits it in two, one parallel group dimension and one smaller reduction dimension.

A grouped 2D-convolution with batch size N , stride 1 and no padding is trivially expressible in TC as:¹³

```
def gconv(float(N,G,C,H,W) I, float(G,F,C,KH,KW) W1,
         float(M) B) → (O) {
    O(n,g,o,h,w) +=! I(n,g,i, h + kh, w + kw)
                    * W1(g,o,i,kh,kw)
    O(n,g,o,h,w) = O(n,g,o,h,w) + B(m)
}
```

Despite TC’s current support for time-domain convolutions only, it still outperforms Caffe2 based on CUDNN Winograd kernels by $1.4\times$ to $3.6\times$ (resp. $1.9\times$ to $8.8\times$ on Pascal). On Maxwell, Caffe2 calls a CUDNN kernel (`maxwell_scudnn_winograd_128x128_ldg1_ldg4_tile228n_nt`) 32 times: this is about $10\times$ better than a few months earlier when it was implemented as 32^2 direct-convolution CUDNN kernel calls; bridging the years spanned between the discovery of an operation and its implementation in a library is one of our main contributions.

Production Models We finish our discussion with a model used in practice at scale. Historically, Multi-Layer Perceptrons (MLPs) are the first neural networks in the literature [56]. In the context of inference—deploying a trained model in production to drive decisions to improve user experience and revenue, based on individual preferences and history—the landscape is heavily shifting to custom hardware where the most serious efficiency gains lie, both in data centers [44, 70] and on mobile devices. Still, these models need to be trained before being deployed. Training usually involves large amounts of time-dependent information such as weather conditions or world events. The training procedure generally involves backpropagation and stochastic gradient descent. For now, the preferred hardware for this task remains clusters of NVIDIA GPUs. Because of the small low-latency nature of these models, default library implementations are not optimal.¹⁴ One specific MLP model—used in some applications at Facebook—is very small by the standards of computer vision pipelines [41]. Batch size is 128, mandated by model training accuracy. Similar models have been proposed in the literature for recommender systems [19] and click through rate prediction [94]. A TC representation for the neural network portion of the model is given in the supplementary material. In the reference Caffe2 implementation, the DNN represents roughly 70% of the time. It consists of 4 sections on which we apply TC: (1) 2 parallel lookup table operators (**2LUT**) for which we can generate a fused kernel, (2) 1 transposed matmul layer, (3) 1 **MLP1** layer (a.k.a. **fcrelu**) which we find beneficial to distribute from the layers below, and (4) 3 MLP layers in a sequence (**MLP3**) for which we generate a single CUDA kernel. The TC for **2LUT** is:

```
def 2LUT(float(E1,D) LUT1, int(B,L1) I1,
         float(E2,D) LUT2, int(B,L2) I2) → (O1, O2) {
    O1(i,j) +=! LUT1(I1(i,k),j)
    O2(i,j) +=! LUT2(I2(i,k),j)
}
```

Lookup Table Embeddings. Large scale embeddings [60] are used as a portable encoding. Concretely, an embedding is a 2-D matrix of numbers. The associated computation performs a sparse lookup

¹²The successor of ResNet [41], winner of the Imagenet 2015 competition.

¹³Incidentally this form is the so-called NCHW layout, because the C and F dimensions in the TC are referred to as channels and filters. Depending on the paper these can also be called input and output channels.

¹⁴In practice, this limitation has become so dire that engineers have expended significant effort writing a multi-GPU, asynchronous, Hogwild [74] version of the model to improve throughput without resorting to fully synchronous minibatch size increase.

from a small subset of rows out of a large table and a reduction on the rows. The sizes of interest are $(E1, E2, D, L1, L2) = (10^7, 10^7, 64, 50, 50)$. We developed a novel 2-stage loading in shared memory (see Section 5.5). Without it, we observe long latency operations that depend upon each other and cripple the overall performance by more than $5\times$. Notice fused **2LUT** performing slightly worse than $2\times 1LUT$. An extra order of parallelism is missing without parallel reduction support. Our synthesized kernel runs $4\times$ (resp. $4.1\times$ on Pascal) faster than the Caffe2 reference, yet the latter relies on the CUB library and uses this extra parallelism.

Transposed Matmul. The transposed matrix multiplication (C3 is with a weight matrix of size $(1000, 1024)$). The same register and reduction support argument applies but for such sizes we are already competitive on Pascal.

Single Multi-Layer Perceptron. The intermediate **MLP1** layer (i.e., **fcrelu**) is not beneficially fused in frameworks with the following layers. We achieve up to $1.5\times$ speedup over CUBLAS on Pascal in spite of missing register optimization.

Fused Multi-Layer Perceptron. Lastly, **MLP3** is a sequence of 3 low-latency MLP layers that feed into the binary classifier. Depending on the ML framework, the underlying HPC library *and the ML user*, one expects to see anywhere between 3 and 9 CUDA kernel calls. *In this low-latency regime, CUDA kernel launch overhead is significant.* In contrast, our JIT flow emits 1 single CUDA kernel call which runs up to $3.6\times$ faster than the Caffe2 reference, based on a mix of CUDNN and CUBLAS. Also note our kernel runs in $32\mu s$ with a mean overhead of $25\mu s$, partly attributable to NVRTC.

8 Perspectives

This work opens numerous research and exploitation opportunities:

1. distribute and share best implementations, as well as autotuning history, for any architecture, via protobuf;
2. port to more architectures, and combine with libraries of primitives for high single-thread performance [79];
3. exploit data layout transformations in a systematic manner and use them both as part of automated tuning and for easily adding support for vector types, in particular on interesting low-precision formats with arbitrary number of bits;
4. implement an automated DAG partitioning algorithm, informed by underlying performance of synthesized kernels;
5. mix Halide-style transformations for algorithmic tiling, model parallelism and model slicing, in combination with advanced loop transformations;
6. provide symbolic automatic differentiation on TC directly;
7. more dynamic control flow and gray-box libraries, implemented through a mechanism similar to PENCIL summaries, as well as dynamic inspection or speculative schemes to hide dependences;
8. extend the data representations to sparse, vector and mixed-precision types;
9. generally, accelerate ML research with both performance and ease of translating a mathematical specification to an actual implementation.

9 Conclusion

We demonstrated an end-to-end flow from the high-level Tensor Comprehensions (TC) language down to automatically generated kernels on GPUs. TC resembles the whiteboard mathematical model of a deep neural network and makes it easy to reason about, communicate, and to manually alter the computations and storage/computation tradeoffs. The language supports a rich syntax of tensor operations while remaining within the realm of polyhedral compiler analysis, affine transformations and (iterated) linear optimization. The flow leverages decades of progress in polyhedral compilation and also implements domain-specific optimizations, code generation, autotuning with a compilation cache, and seamless integration with Caffe2 and PyTorch through the ATen tensor library.

TC quickly synthesizes solid baseline versions that effectively lift bottlenecks in large training runs. In practice, when such bottlenecks arise, ML research slows down sometimes significantly, and serious engineering efforts need to be mobilized. Our contribution addresses this productivity and efficiency gap; it brings more expressive power and control in the hands of domain experts, relieving dependence of ML frameworks on highly tuned vendor libraries without compromising performance. TC also automates much boilerplate that has been replicated over the numerous deep learning frameworks, and builds on a generic polyhedral intermediate representation and libraries shared with other domains (image processing) and general-purpose compilers (LLVM/Polly).

Acknowledgements We are grateful for the numerous discussions and fruitful ongoing collaboration with the following people: Tianqi Chen, Moustapha Cissé, Cijo Jose, Chandan Reddy, Will Feng, Edward Yang, Léon Bottou, Tobias Grosser, Dmytro Dzhulgakov, and Yangqing Jia. This work was partly supported by the Swiss National Science Foundation in the context of grant PZ00P2_168016.

References

- [1]M. Abadi, P. Barham, J. Chen, Z. Chen, A. Davis, J. Dean, M. Devin, S. Ghemawat, G. Irving, M. Isard, et al. TensorFlow: A system for large-scale machine learning. In *OSDI*, volume 16, pages 265–283, 2016.
- [2]S. G. Andrew Lavin. Fast algorithms for convolutional neural networks. *CoRR*, abs/1509.09308, 2015, 1509.09308.
- [3]R. Baghdadi, U. Beaugnon, A. Cohen, T. Grosser, M. Kruse, C. Reddy, S. Verdoolaege, A. Betts, A. F. Donaldson, J. Ketema, J. Absar, S. v Haastregt, A. Kravets, A. Lokhmotov, R. David, and E. Hajiye. PENCIL: A Platform-Neutral Compute Intermediate Language for Accelerator Programming. In *2015 International Conference on Parallel Architecture and Compilation (PACT)*, pages 138–149, Oct. 2015.
- [4]L. Bagnères, O. Zinenko, S. Huot, and C. Bastoul. Opening Polyhedral Compiler’s Black Box. In *Proceedings of the 2016 International Symposium on Code Generation and Optimization, CGO 2016*, pages 128–138, New York, NY, USA, 2016. ACM.
- [5]M. M. Baskaran, U. Bondhugula, S. Krishnamoorthy, J. Ramanujam, A. Rountev, and P. Sadayappan. A compiler framework for optimization of affine loop nests for GPGPUs. In *Proceedings of the 22Nd Annual International Conference on Supercomputing, ICS ’08*, pages 225–234, New York, NY, USA, 2008. ACM.
- [6]C. Bastoul. Code Generation in the Polyhedral Model Is Easier Than You Think. In *Proceedings of the 13th International Conference on Parallel Architectures and Compilation Techniques, PACT ’04*, pages 7–16, Washington, DC, USA, 2004. IEEE Computer Society.
- [7]U. Beaugnon, A. Kravets, S. van Haastregt, R. Baghdadi, D. Tweed, J. Absar, and A. Lokhmotov. Vobla: A vehicle for optimized basic linear algebra. In *Proceedings of the 2014 SIGPLAN/SIGBED Conference on Languages, Compilers and Tools for Embedded Systems, LCTES ’14*, pages 115–124, New York, NY, USA, 2014. ACM.
- [8]O. Beckmann, A. Houghton, P. H. J. Kelly, and M. Mellor. Run-time code generation in C++ as a foundation for domain-specific optimisation. In *Proceedings of the 2003 Dagstuhl Workshop on Domain-Specific Program Generation*, 2003.
- [9]G. Belter, E. R. Jessup, I. Karlin, and J. G. Siek. Automating the generation of composed linear algebra kernels. In *Proceedings of the Conference on High Performance Computing Networking, Storage and Analysis, SC ’09*, pages 59:1–59:12, New York, NY, USA, 2009. ACM.
- [10]M.-W. Benabderrahmane, L.-N. Pouchet, A. Cohen, and C. Bastoul. The Polyhedral Model Is More Widely Applicable Than You Think. In R. Gupta, editor, *Compiler Construction*, number 6011 in Lecture Notes in Computer Science, pages 283–303. Springer, Mar. 2010.
- [11]U. Bondhugula, A. Acharya, and A. Cohen. The Pluto+ Algorithm: A Practical Approach for Parallelization and Locality Optimization of Affine Loop Nests. *ACM Transactions on Programming Languages and Systems*, 38(3):12:1–12:32, Apr. 2016.
- [12]U. Bondhugula, A. Hartono, J. Ramanujam, and P. Sadayappan. A Practical Automatic Polyhedral Parallelizer and Locality Optimizer. *ACM SIGPLAN Notices*, 43(6):101–113, 2008.
- [13]L. Bottou and Y. LeCun. Lush reference manual. <http://lush.sf.net/doc.html>, 2002.

- [14]C. Chen. Polyhedra Scanning Revisited. In *Proceedings of the 33rd ACM SIGPLAN Conference on Programming Language Design and Implementation*, PLDI '12, pages 499–508, New York, NY, USA, 2012. ACM.
- [15]C. Chen, J. Chame, and M. Hall. Chill: A framework for composing high-level loop transformations. Technical report, Technical Report 08-897, U. of Southern California, 2008.
- [16]T. Chen. TVM. <http://tvm-lang.org/2017/08/17/tvm-release-announcement.html>, Aug. 2017.
- [17]T. Chen, M. Li, Y. Li, M. Lin, N. Wang, M. Wang, T. Xiao, B. Xu, C. Zhang, and Z. Zhang. MXNet: A flexible and efficient machine learning library for heterogeneous distributed systems. *CoRR*, abs/1512.01274, 2015, 1512.01274.
- [18]T. Chen, T. Moreau, Z. Jiang, H. Shen, E. Yan, L. Wang, Y. Hu, L. Ceze, C. Guestrin, and A. Krishnamurthy. TVM: End-to-end optimization stack for deep learning, 2018, arXiv:1802.04799.
- [19]H. Cheng, L. Koc, J. Harmsen, T. Shaked, T. Chandra, H. Aradhye, G. Anderson, G. Corrado, W. Chai, M. Ispir, R. Anil, Z. Haque, L. Hong, V. Jain, X. Liu, and H. Shah. Wide & deep learning for recommender systems. *CoRR*, abs/1606.07792, 2016, 1606.07792.
- [20]F. Chollet et al. Keras. <https://github.com/fchollet/keras>, 2015.
- [21]D. C. Ciresan, U. Meier, L. M. Gambardella, and J. Schmidhuber. Deep big simple neural nets excel on handwritten digit recognition. *CoRR*, abs/1003.0358, 2010, 1003.0358.
- [22]A. Cohen, S. Donadio, M. J. Garzarán, C. Herrmann, O. Kiselyov, and D. Padua. In search of a program generator to implement generic transformations for high-performance computing. *Science of Computer Programming*, 62(1):25–46, Sept. 2006. Special issue on the First MetaOCaml Workshop 2004.
- [23]A. Cohen, S. Girbal, D. Parelo, M. Sigler, O. Temam, and N. Vasilache. Facilitating the search for compositions of program transformations. In *ACM Intl. Conf. on Supercomputing (ICS)*, pages 151–160, Boston, Massachusetts, June 2005.
- [24]R. Collobert, K. Kavukcuoglu, and C. Farabet. Implementing neural networks efficiently. In G. Montavon, G. Orr, and K.-R. Muller, editors, *Neural Networks: Tricks of the Trade*. Springer, 2012.
- [25]S. Donadio, J. Brodman, T. Roeder, K. Yotov, D. Barthou, A. Cohen, M. J. Garzarán, D. Padua, and K. Pingali. A language for the compact representation of multiple program versions. In *Languages and Compilers for Parallel Computing (LCPC)*, LNCS, Hawthorne, New York, Oct. 2005. Springer. 15 pages.
- [26]M. Dukhan. Peachpy: A python framework for developing high-performance assembly kernels. In *Proceedings of the 3rd Workshop on Python for High Performance and Scientific Computing*, 2013.
- [27]P. Feautrier. Dataflow Analysis of Array and Scalar References. *International Journal of Parallel Programming*, 20(1):23–53, 1991.
- [28]P. Feautrier. Some Efficient Solutions to the Affine Scheduling Problem. Part II. Multidimensional Time. *International Journal of Parallel Programming*, 21(6):389–420, 1992.
- [29]P. Feautrier and C. Lengauer. Polyhedron Model. In D. Padua, editor, *Encyclopedia of Parallel Computing*, pages 1581–1592. Springer, 2011.
- [30]B. B. Fraguera, G. Bikshandi, J. Guo, M. J. Garzarn, D. Padua, and C. von Praun. Optimization techniques for efficient hta programs. *Parallel Computing*, 38(9):465 – 484, 2012.
- [31]M. Frigo and S. G. Johnson. FFTW: An adaptive software architecture for the FFT. In *Acoustics, Speech and Signal Processing, 1998. Proceedings of the 1998 IEEE International Conference on*, volume 3, pages 1381–1384. IEEE, 1998.
- [32]S. Girbal, N. Vasilache, C. Bastoul, A. Cohen, D. Parelo, M. Sigler, and O. Temam. Semi-Automatic Composition of Loop Transformations for Deep Parallelism and Memory Hierarchies. *International Journal of Parallel Programming*, 34(3):261–317, July 2006. URUK.
- [33]D. E. Goldberg. *Genetic Algorithms in Search, Optimization and Machine Learning*. Addison-Wesley Longman Publishing Co., Inc., Boston, MA, USA, 1st edition, 1989.
- [34]D. Golovin, B. Solnik, S. Moitra, G. Kochanski, J. E. Karro, and D. Sculley, editors. *Google Vizier: A Service for Black-Box Optimization*, 2017.

- [35] Protocol buffers developer guide. <https://developers.google.com/protocol-buffers/docs/overview>, 2017.
- [36] XLA: Domain-specific compiler for linear algebra to optimizes tensorflow computations. <https://www.tensorflow.org/performance/xla>, 2017. commit 0f1b88a.
- [37] P. Goyal, P. Dollár, R. B. Girshick, P. Noordhuis, L. Wesolowski, A. Kyrola, A. Tulloch, Y. Jia, and K. He. Accurate, large minibatch SGD: training ImageNet in 1 hour. *CoRR*, abs/1706.02677, 2017, 1706.02677.
- [38] S. Gray. Maxas: assembler for Nvidia Maxwell architecture. <https://github.com/NervanaSystems/maxas>, 2014.
- [39] T. Grosser, S. Verdoolaege, and A. Cohen. Polyhedral AST Generation Is More Than Scanning Polyhedra. *ACM Transactions on Programming Languages and Systems*, 37(4):12:1–12:50, July 2015.
- [40] V. Grover. personal communication, 2017.
- [41] K. He, X. Zhang, S. Ren, and J. Sun. Deep residual learning for image recognition. *CoRR*, abs/1512.03385, 2015, 1512.03385.
- [42] G. E. Hinton, N. Srivastava, A. Krizhevsky, I. Sutskever, and R. Salakhutdinov. Improving neural networks by preventing co-adaptation of feature detectors. *CoRR*, abs/1207.0580, 2012, 1207.0580.
- [43] J. Johnson. Pytorch examples. <https://github.com/jcjohnson/pytorch-examples>, 2015. commit 0f1b88a.
- [44] N. P. Jouppi, C. Young, N. Patil, D. Patterson, G. Agrawal, R. Bajwa, S. Bates, S. Bhatia, N. Boden, A. Borchers, R. Boyle, P. Cantin, C. Chao, C. Clark, J. Coriell, M. Daley, M. Dau, J. Dean, B. Gelb, T. V. Ghaemmaghami, R. Gottipati, W. Gulland, R. Hagmann, C. R. Ho, D. Hogberg, J. Hu, R. Hundt, D. Hurt, J. Ibarz, A. Jaffey, A. Jaworski, A. Kaplan, H. Khaitan, D. Killebrew, A. Koch, N. Kumar, S. Lacy, J. Laudon, J. Law, D. Le, C. Leary, Z. Liu, K. Lucke, A. Lundin, G. MacKean, A. Maggiore, M. Mahony, K. Miller, R. Nagarajan, R. Narayanaswami, R. Ni, K. Nix, T. Norrie, M. Omernick, N. Penukonda, A. Phelps, J. Ross, M. Ross, A. Salek, E. Samadiani, C. Severn, G. Sizikov, M. Snellman, J. Souter, D. Steinberg, A. Swing, M. Tan, G. Thorson, B. Tian, H. Toma, E. Tuttle, V. Vasudevan, R. Walter, W. Wang, E. Wilcox, and D. H. Yoon. In-datacenter performance analysis of a tensor processing unit. In *Proceedings of the 44th Annual International Symposium on Computer Architecture, ISCA 2017, Toronto, ON, Canada, June 24-28, 2017*, pages 1–12, 2017.
- [45] K. Kennedy and J. R. Allen. *Optimizing Compilers for Modern Architectures: A Dependence-Based Approach*. Morgan Kaufmann Publishers Inc., San Francisco, CA, USA, 2002.
- [46] F. Kjolstad, S. Kamil, S. Chou, D. Lugato, and S. Amarasinghe. The tensor algebra compiler. *Proc. ACM Program. Lang.*, 1(OOPSLA):77:1–77:29, Oct. 2017.
- [47] F. Kjolstad, S. Kamil, J. Ragan-Kelley, D. I. W. Levin, S. Sueda, D. Chen, E. Vouga, D. M. Kaufman, G. Kanwar, W. Matusik, and S. Amarasinghe. Simit: A language for physical simulation. *ACM Trans. Graph.*, 35(2):20:1–20:21, Mar. 2016.
- [48] A. Klöckner. Loo.py: transformation-based code generation for gpus and cpus. *CoRR*, abs/1405.7470, 2014, 1405.7470. Proc. of ARRAY 2014: ACM SIGPLAN Workshop on Libraries, Languages, and Compilers for Array Programming.
- [49] M. Kong, R. Veras, K. Stock, F. Franchetti, L. Pouchet, and P. Sadayappan. When polyhedral transformations meet SIMD code generation. In *ACM SIGPLAN Conference on Programming Language Design and Implementation, PLDI '13, Seattle, WA, USA, June 16-19, 2013*, pages 127–138, 2013.
- [50] A. Krizhevsky, I. Sutskever, and G. E. Hinton. ImageNet classification with deep convolutional neural networks. In F. Pereira, C. J. C. Burges, L. Bottou, and K. Q. Weinberger, editors, *Advances in Neural Information Processing Systems 25*, pages 1097–1105. Curran Associates, Inc., 2012.
- [51] H. Le Verge, C. Mauras, and P. Quinton. The ALPHA language and its use for the design of systolic arrays. *Journal of VLSI signal processing systems for signal, image and video technology*, 3(3):173–182, Sep 1991.

- [52]Y. LeCun, B. E. Boser, J. S. Denker, D. Henderson, R. E. Howard, W. E. Hubbard, and L. D. Jackel. Handwritten digit recognition with a back-propagation network. In *Advances in Neural Information Processing Systems 2, [NIPS Conference, Denver, Colorado, USA, November 27-30, 1989]*, pages 396–404, 1989.
- [53]M. Luján, T. L. Freeman, and J. R. Gurd. Oolala: An object oriented analysis and design of numerical linear algebra. In *Proceedings of the 15th ACM SIGPLAN Conference on Object-oriented Programming, Systems, Languages, and Applications, OOPSLA '00*, pages 229–252, New York, NY, USA, 2000. ACM.
- [54]B. Meister, N. Vasilache, D. Wohlford, M. M. Baskaran, A. Leung, and R. Lethin. *R-Stream Compiler*, pages 1756–1765. Springer, Boston, MA, 2011.
- [55]Microsoft unveils project brainwave for real-time ai. <https://www.microsoft.com/en-us/research/blog/microsoft-unveils-project-brainwave>, Aug. 2017.
- [56]M. L. Minsky and S. Papert. *Perceptrons: an introduction to computational geometry; 1st ed.* MIT, Cambridge, MA, 1969.
- [57]R. T. Mullapudi, A. Adams, D. Sharlet, J. Ragan-Kelley, and K. Fatahalian. Automatically scheduling halide image processing pipelines. *ACM Transactions on Graphics (TOG)*, 35(4):83, 2016.
- [58]R. T. Mullapudi, A. Adams, D. Sharlet, J. Ragan-Kelley, and K. Fatahalian. Automatically scheduling halide image processing pipelines. *ACM Trans. Graph.*, 35(4):83:1–83:11, July 2016.
- [59]R. T. Mullapudi, V. Vasista, and U. Bondhugula. Polymage: Automatic optimization for image processing pipelines. In *Proceedings of the Twentieth International Conference on Architectural Support for Programming Languages and Operating Systems, ASPLOS '15*, pages 429–443, New York, NY, USA, 2015. ACM.
- [60]M. Nickel, K. Murphy, V. Tresp, and E. Gabrilovich. A review of relational machine learning for knowledge graphs. *Proceedings of the IEEE*, 104(1):11–33, 2016.
- [61]F. Nielson, H. Nielson, and C. Hankin. *Principles of Program Analysis*. Springer, 1999.
- [62]Deploying deep neural networks with Nvidia TensorRT. <https://devblogs.nvidia.com/parallelforall/deploying-deep-learning-nvidia-tensorrt>, Apr. 2017.
- [63]Inside Volta: The worlds most advanced data center GPU. <https://devblogs.nvidia.com/parallelforall/inside-volta>, May 2017.
- [64]M. Pacula, J. Ansel, S. Amarasinghe, and U.-M. O'Reilly. *Hyperparameter Tuning in Bandit-Based Adaptive Operator Selection*, pages 73–82. Springer, Berlin, Heidelberg, 2012.
- [65]L.-N. Pouchet, U. Bondhugula, C. Bastoul, A. Cohen, J. Ramanujam, P. Sadayappan, and N. Vasilache. Loop transformations: Convexity, pruning and optimization. In *38th ACM Symp. on Principles of Programming Languages (POPL)*, Austin, Texas, Jan. 2011.
- [66]L.-N. Pouchet, P. Zhang, P. Sadayappan, and J. Cong. Polyhedral-based data reuse optimization for configurable computing. In *Proceedings of the ACM/SIGDA International Symposium on Field Programmable Gate Arrays, FPGA '13*, pages 29–38, New York, NY, USA, 2013. ACM.
- [67]B. Pradelle, B. Meister, M. Baskaran, J. Springer, and R. Lethin. Polyhedral optimization of tensorflow computation graphs. In *6th Workshop on Extreme-scale Programming Tools (ESPT, associated with SC'17)*, Nov. 2017.
- [68]W. Pugh and D. Wonnacott. Static Analysis of Upper and Lower Bounds on Dependences and Parallelism. *ACM Trans. Program. Lang. Syst.*, 16(4):1248–1278, July 1994.
- [69]M. Püschel, J. M. F. Moura, B. Singer, J. Xiong, J. Johnson, D. Padua, M. Veloso, and R. W. Johnson. Spiral: A generator for platform-adapted libraries of signal processing algorithms. *The International Journal of High Performance Computing Applications*, 18(1):21–45, 2004.
- [70]A. Putnam, A. Caulfield, E. Chung, D. Chiou, K. Constantinides, J. Demme, H. Esmaeilzadeh, J. Fowers, J. Gray, M. Haselman, S. Hauck, S. Heil, A. Hormati, J.-Y. Kim, S. Lanka, E. Peterson, A. Smith, J. Thong, P. Y. Xiao, D. Burger, J. Larus, G. P. Gopal, and S. Pope. A reconfigurable fabric for accelerating large-scale datacenter services. In *Proceeding of the 41st Annual International Symposium on Computer Architecture (ISCA)*, pages 13–24. IEEE Press, June 2014.

- [71]PyTorch: Tensors and dynamic neural networks in python with strong GPU acceleration. <https://pytorch.org>, 2017.
- [72]J. Ragan-Kelley, C. Barnes, A. Adams, S. Paris, F. Durand, and S. Amarasinghe. Halide: a language and compiler for optimizing parallelism, locality, and recomputation in image processing pipelines. *ACM SIGPLAN Notices*, 48(6):519–530, 2013.
- [73]R. Raina, A. Madhavan, and A. Y. Ng. Large-scale deep unsupervised learning using graphics processors. In *Proceedings of the 26th Annual International Conference on Machine Learning, ICML '09*, pages 873–880, New York, NY, USA, 2009. ACM.
- [74]B. Recht, C. Re, S. Wright, and F. Niu. Hogwild: A lock-free approach to parallelizing stochastic gradient descent. In J. Shawe-Taylor, R. S. Zemel, P. L. Bartlett, F. Pereira, and K. Q. Weinberger, editors, *Advances in Neural Information Processing Systems 24*, pages 693–701. Curran Associates, Inc., 2011.
- [75]S. Rendle. Factorization machines. In *Proceedings of the 2010 IEEE International Conference on Data Mining, ICDM '10*, pages 995–1000, Washington, DC, USA, 2010. IEEE Computer Society.
- [76]T. Rompf and M. Odersky. Lightweight modular staging: A pragmatic approach to runtime code generation and compiled dsls. In *Proceedings of the Ninth International Conference on Generative Programming and Component Engineering, GPCE '10*, pages 127–136, New York, NY, USA, 2010. ACM.
- [77]M. D. Smith. Overcoming the challenges to feedback-directed optimization (keynote talk). In *Proceedings of the ACM SIGPLAN Workshop on Dynamic and Adaptive Compilation and Optimization, DYNAMO '00*, pages 1–11, New York, NY, USA, 2000. ACM.
- [78]J. Snoek, H. Larochelle, and R. P. Adams. Practical bayesian optimization of machine learning algorithms. In *Proceedings of the 25th International Conference on Neural Information Processing Systems - Volume 2, NIPS'12*, pages 2951–2959, USA, 2012. Curran Associates Inc.
- [79]D. G. Spampinato and M. Püschel. A basic linear algebra compiler for structured matrices. In *Proceedings of the 2016 International Symposium on Code Generation and Optimization, CGO 2016, Barcelona, Spain, March 12-18, 2016*, pages 117–127, 2016.
- [80]K. Stock, T. Henretty, I. Murugandi, P. Sadayappan, and R. Harrison. Model-driven SIMD code generation for a multi-resolution tensor kernel. In *2011 IEEE International Parallel & Distributed Processing Symposium (IPDPS)*, pages 1058–1067. IEEE, 2011.
- [81]Theano Development Team. Theano: A Python framework for fast computation of mathematical expressions. *arXiv e-prints*, abs/1605.02688, May 2016.
- [82]L. Truong, R. Barik, E. Totoni, H. Liu, C. Markley, A. Fox, and T. Shpeisman. Latte: A language, compiler, and runtime for elegant and efficient deep neural networks. In *Proceedings of the 37th ACM SIGPLAN Conference on Programming Language Design and Implementation, PLDI '16*, pages 209–223, New York, NY, USA, 2016. ACM.
- [83]N. Vasilache, J. Johnson, M. Mathieu, S. Chintala, S. Piantino, and Y. LeCun. Fast convolutional nets with fbfft: A GPU performance evaluation. *CoRR*, abs/1412.7580, 2014.
- [84]N. Vasilache, B. Meister, M. Baskaran, and R. Lethin. Joint scheduling and layout optimization to enable multi-level vectorization. In *IMPACT-2: 2nd International Workshop on Polyhedral Compilation Techniques*, Paris, France, Jan 2012.
- [85]T. Veldhuizen and E. Gannon. Active libraries: Rethinking the roles of compilers and libraries. In M. E. Henderson, C. R. Anderson, and S. L. Lyons, editors, *Proceedings of the 1998 SIAM Workshop: Object Oriented Methods for Interoperable Scientific and Engineering Computing*, pages 286–295. SIAM Press, 1998.
- [86]S. Verdoolaege. Isl: An integer set library for the polyhedral model. In *Proceedings of the Third International Congress Conference on Mathematical Software, ICMS'10*, pages 299–302, Berlin, Heidelberg, 2010. Springer.
- [87]S. Verdoolaege. Counting Affine Calculator and Applications. In *First International Workshop on Polyhedral Compilation Techniques (IMPACT'11)*, Chamonix, France, Apr. 2011.
- [88]S. Verdoolaege, J. Carlos Juega, A. Cohen, J. Ignacio Gómez, C. Tenllado, and F. Catthoor. Polyhedral Parallel Code Generation for CUDA. *ACM Transactions on Architecture and Code Optimization*, 9(4):54:1–54:23, Jan. 2013.

- [89]S. Verdoolaege and T. Grosser. Polyhedral extraction tool. In *In Second International Workshop on Polyhedral Compilation Techniques (IMPACT12)*, 2012.
- [90]S. Verdoolaege, S. Guelton, T. Grosser, and A. Cohen. Schedule Trees. In *4th Workshop on Polyhedral Compilation Techniques (IMPACT, Associated with HiPEAC)*, page 9, Vienna, Austria, Jan. 2014.
- [91]S. Verdoolaege and G. Janssens. Scheduling for PPCG. Report CW 706, Department of Computer Science, KU Leuven, Leuven, Belgium, June 2017.
- [92]R. C. Whaley and J. J. Dongarra. Automatically tuned linear algebra software. In *Proceedings of the 1998 ACM/IEEE Conference on Supercomputing, SC '98*, pages 1–27, Washington, DC, USA, 1998. IEEE Computer Society.
- [93]S. Xie, R. B. Girshick, P. Dollár, Z. Tu, and K. He. Aggregated residual transformations for deep neural networks. *CoRR*, abs/1611.05431, 2016, 1611.05431.
- [94]G. Zhou, C. Song, X. Zhu, X. Ma, Y. Yan, X. Dai, H. Zhu, J. Jin, H. Li, and K. Gai. Deep Interest Network for Click-Through Rate Prediction. *ArXiv e-prints*, June 2017, 1706.06978.
- [95]O. Zinenko, S. Verdoolaege, C. Reddy, J. Shirako, T. Grosser, V. Sarkar, and A. Cohen. Unified Polyhedral Modeling of Temporal and Spatial Locality. Technical Report RR-9110, Inria, Paris, France, Oct 2017.

A Appendix

This supplementary material collects technical detail useful to provide complete coverage of the proposed methods.

Figure 14 shows the grammar of the Tensor Comprehension language in EBNF notation.

A.1 ML Frameworks of Interest

We discuss TensorFlow at its core level: mathematical operators, as described originally [1]. Additional higher-level abstractions such as those in Keras [20] and in TensorFlow itself (e.g., `tf-fold` and `tf-eager`) improve programmability building upon these operators. TensorFlow (along with most other ML frameworks) is used to describe and perform computations on n -dimensional tensors. Computation on tensors is described via *operators*, which take a set of input tensors and define a set of output tensors as described by a mathematical operation on the input tensors. Using an initial set of tensors (which may include placeholder or variable tensors), the programmer composes operators into a static acyclic dataflow graph called the DAG. After constructing this DAG, the programmer specifies computations for the graph to run. Most commonly, one specifies a series of steps of a gradient descent. The sample code in Figure 8 gives a feel for using this framework.

Caffe2 [37] is structurally close in design to TensorFlow, albeit with a lighter API and making access to the intermediate results in the computation graph much easier. A major design difference is that Caffe2 assumes intermediate objects to be not only tensors but other opaque data structures, such as AFCS pre-packed matrices of custom layout, or handles to data structures in specialized hardware. This improves portability across different platforms (such as mobile) and interoperability with optimization libraries that may require custom storage formats. Equivalent syntax for Caffe2 is given in Figure 9.

PyTorch [71] shares many abstraction similarities with TensorFlow and Caffe2, with one major exception: the static computation graph. Whereas in frameworks such as TensorFlow and Caffe2, the programmer needs to explicitly specify the computation to be performed and then later execute the computation (potentially given some parameters), PyTorch runs the computation as it is specified. Equivalent syntax for PyTorch is given in Figure 10.

MXNet [17] also shares similar abstractions and offers different paradigms: declarative like Caffe2 and TensorFlow as well as imperative like PyTorch. MXNet also supports multiple languages, Python still being the dominant one. Interestingly, MXNet added compiler abstractions and passes at the core of the toolchain. NNVM is the name of the graph-based intermediate representation (IR) which allows performing graph-rewriting transformations (e.g., for coarsening of library calls and exploring tradeoffs between kernel efficiency and asynchrony like TensorRT [62]). NNVM also allows cutting pieces of the graph and delegating those to TVM [16, 18], a declarative kernel and transformation specification based on Halide [72].

A number of tensor manipulation ideas underlying modern ML frameworks were first implemented by the Lush/SN3 [13] system in the 1990s. The Lush construct `idx-bloop` iterates on the first indices of a collection of tensors. Index arithmetic is achieved by preparing the tensor descriptors with helper functions that manipulate the strides associated with each index. For instance, to implement the “lowering” of convolutions, the `unfold` function returns a new tensor descriptor with an additional dimension that scans each of the overlapping convolution windows. The Lush compiler only performs minor optimizations on such loops: tiling and reordering is left to the user.

A.2 ML Framework Interface API

We expose tensor comprehensions to ML frameworks with an embedded language API similar to libraries for regular expressions, SQL queries, or graphics shading languages. The code is loaded as a string into an execution engine that manages compilation and execution, as shown in Figure 11. This code can then be run which invokes the JIT compiler and autotuner, as shown in Figure 12. This version of the API is specific to Python and PyTorch, but similar APIs exist for C++ and for other ML frameworks such as Caffe2.

Each of these APIs is just a small wrapper around a core framework-agnostic API shown in Figure 13.

```

# 1. Construct a graph representing the model.
x = tf.placeholder(tf.float32, [BATCH, 20])
y = tf.placeholder(tf.float32, [BATCH, 10])
w = tf.Variable(tf.random_uniform([20, 10]))
b = tf.Variable(tf.zeros([10]))
z = tf.nn.relu(tf.matmul(x, w) + b)

# 2. Add nodes to define the optimization algorithm.
loss = tf.nn.softmax_cross_entropy_with_logits(z, y)
opt = tf.train.GradientDescentOptimizer(0.1)
train_op = opt.minimize(loss)

# 3. Execute the computation graph on data.
with tf.Session() as sess:
    sess.run(tf.initialize_all_variables())
    for step in range(NUM_STEPS):
        sess.run(train_op, {x: x_data, y: y_data})

```

Figure 8: Tensorflow code for training a neural network with one fully-connected layer (adapted from [1])

```

# 1. Construct a graph representing the model.
model = model_helper.ModelHelper(name="train")
x, y = model.net.AddExternalInputs('x', 'y')
w = model.param_init_net.UniformFill([], 'w', shape=[20, 10])
b = model.param_init_net.ConstantFill([], 'b', shape=[10])
z = model.net.Relu([model.net.Add([
    model.net.MatMul([x, w], 'z0'), b], 'z1')], 'z')

# 2. Add nodes to define the optimization algorithm.
pred = model.net.Softmax(z, 'pred')
loss = model.net.LabelCrossEntropy([pred, y], 'loss')
model.AddGradientOperators([loss])
optimizer.build_sgd(model, base_learning_rate=0.1, policy="step")

# 3. Execute the computation graph on data.
workspace.RunNetOnce(model.param_init_net)
workspace.CreateNet(model.net)
for i in range(NUM_STEPS):
    workspace.RunNet(model.net.Proto().name)

```

Figure 9: Caffe2 code for training a neural network with one fully-connected layer

```

dtype = torch.FloatTensor
x = Variable(x_data, requires_grad=False)
y = Variable(y_data, requires_grad=False)
w = Variable(torch.randn(20, 10).type(dtype), requires_grad=True)
b = Variable(torch.randn(10).type(dtype), requires_grad=True)

learning_rate = 1e-6
for t in range(500):
    y_pred = (x.mm(w)+b).clamp(min=0)
    loss = (y_pred - y).pow(2).sum()
    loss.backward()
    w.data -= learning_rate * w.grad.data
    b.data -= learning_rate * b.grad.data

    w.grad.data.zero_()
    b.grad.data.zero_()

```

Figure 10: PyTorch code for training a neural network with one fully-connected layer (from Johnson's sample code [43])

```

import tc
ee = tc.ExecutionEngine()
ee.define("""
    def mm(float(M,K) A,
           float(K,N) B) -> (C) {
        C(m,n) +=! A(m,kk) * B(kk,n)
    }
""")

```

Figure 11: Build execution engine

```

import torch
A = torch.randn(3,4)
B = torch.randn(4,5)
C = ee.mm(A, B)

```

Figure 12: JIT compile, tune, or hit the compilation cache, then run

A.3 Background on Polyhedral Compilation

Iteration Domains The polyhedral framework operates on individual loop iterations referred to as *statement instances*. These instances are identified by points in a multidimensional vector space whose coordinates correspond to values of induction variables in the enclosing loops. Constrained by affine bounds, the set of these points, referred to as the *iteration domain*, forms a convex polyhedron, hence the name of the model. In the context of TC, a statement instance is identified by values of all loop iteration variables that appear in a statement. The iteration domains are obtained by inferring the ranges of all iterators following the semantics described in Section 3. Consider again the **sgemm** operation in Figure 1. For the sake of brevity, we refer to the initialization statement (line 2) as S and to the update statement (line 3) as T . The iteration domain for **sgemm** is then described by the union of sets $(N, M, K) \rightarrow \{S(i, j) : 0 \leq i < N \wedge 0 \leq j < K\} \cup \{T(i, j, k) : 0 \leq i < N \wedge 0 \leq j < K \wedge 0 \leq k < M\}$.

Schedules The points of the *iteration domain* are traversed in the lexicographical order of their logical execution dates. Conventionally, these dates are defined *via* a closed-form *schedule* that associates a date to each point. The main part of the paper sketches the more specific schedule tree representation used in this work.

Code Generation Given an iteration domain and a schedule, one can generate a sequence of loop nests that visits all iteration domain points in the order imposed by the schedule. Efficient algorithms exist to generate FORTRAN, C + OpenMP, CUDA or OpenCL code [6, 14, 88]. *isl*’s state of the art algorithm generates an abstract syntax tree, which can be traversed to match any imperative syntax [39].

Representing and Preserving Dependences One distinctive advantage of the polyhedral framework resides in its *relational abstraction of dependences* described as unions of piecewise affine relations—i.e., not necessarily convex or uniform, with the ability to conduct both exact and conservative/approximate instance-wise dependence analysis. This analysis ensures that schedule tree modifications preserve the program semantics. It is based on *access relations* that associate statement instances to the data they access, in our case—tensor elements. Access relations use named tuples to identify tensors and are classified according to the access direction: read or write. For the update statement in the **sgemm** example, the write access relation is $\mathcal{A}_{\text{write}} = (N, M, K) \rightarrow \{T(i, j, k) \rightarrow C(i, j)\}$ and the read access (union of) relation(s) is $\mathcal{A}_{\text{read}} = (N, M, K) \rightarrow \{T(i, j, k) \rightarrow A(i, k)\} \cup \{T(i, j, k) \rightarrow B(k, j)\} \cup \{T(i, j, k) \rightarrow C(i, j)\} \cup \{T(i, j, k) \rightarrow a()\}$.

Dependence Analysis A *dependence* exists between two statement instances that access the same tensor element if at least one of them writes to that element. For two schedules to give the program identical semantics, it is sufficient that both of them sequence pairs of dependent instances in the same relative order. Therefore, a program transformation that preserves or *respects* the dependences is considered *valid*. A dependence relation can be obtained by composing (inverse) access relations and restricting them according to the schedule. For example, a flow dependence is expressed as $\{(D_1 \rightarrow D_2) \mid (D_1 \rightarrow D_2) \subset A_{\text{read}, D_2} \circ A_{\text{write}, D_1}^{-1} \wedge S(D_1) \prec S(D_2)\}$, where D_1, D_2 are iteration domain spaces and S is the schedule. In the **sgemm** case, there exists, among others, a flow dependence between the initialization and the update statements, defined by $(N, M, K) \rightarrow \{S(i, j) \rightarrow T(i', j', k) \mid i' = i \wedge j' = j \wedge 0 \leq i, i' < N \wedge 0 \leq j, j' < K \wedge 0 \leq k < M\}$. The

```

struct TensorInfo {
    DLDataType type;
    std::vector<int64_t> shape;
    std::vector<int64_t> strides;
};

class ExecutionEngine {
public:
    ExecutionEngine() = default;

    // create the funcDB_ using the language passed to it
    // supports multiple TCs
    void define(const std::string& language);

    // get the output Tensor info that can be used by the
    // calling framework to allocate storage for the output
    std::vector<TensorInfo> inferOutputTensorInfo(
        const std::string& name,
        const std::vector<const DLTensor*>& inTensorPtrs);

    // Returns a handle for the compiled kernel
    size_t compile(
        const std::string& name,
        const std::vector<const DLTensor*>& inputs,
        const std::vector<DLTensor*>& outputs,
        const IslKernelOptions& options);

    // Run a TC specified by its name on the given tensor
    // inputs and fill the outputs with the result.
    // The TC is looked up by its handle, sanity checks are
    // performed on name and input / output sizes.
    // If profile is set, the kernel runtime is returned.
    Duration run(
        const std::string& name,
        const std::vector<const DLTensor*>& inputs,
        const std::vector<DLTensor*>& outputs,
        size_t handle,
        bool profile = false);

private:
    struct ExecutorInfo {...};

    // Mutex to support multi-threaded autotuner interaction
    std::mutex executorInfoMutex;
    std::vector<std::unique_ptr<ExecutorInfo>> executors_;
    std::map<std::string, tc::TreeRef> tcNameMap_;
    size_t handleCounter = 0;
};

```

Figure 13: All libraries that expose tensor comprehensions go through a framework-agnostic API for loading and running code; to exchange tensor data, the API uses DLTensor, a common interchange format for in-memory tensor data

schedule tree presented in Figure 3.a schedules $S(i, j)$ before any $T(i, j, k)$ thanks to a Sequence node, respecting the dependence and making the transformation valid.

The previous expression corresponds to the simplest, *memory-based* dependence analysis, which considers two instances to be dependent if they access the same memory location. It can be further refined by performing exact *data-flow analysis* [27], considering only the instance-wise def-use pairs (a.k.a. sources and sinks). This refinement will result in the flow dependence between `sgemm` statements to be restricted to instances $T(i, j, k = 0)$. In *isl*, dependence analysis also distinguishes *potential* (may) accesses from *definite* (must) accesses. The distinction occurs, e.g., when modeling indirect or otherwise non-affine accesses; such accesses are treated as potentially accessing all possible elements along the given tensor dimension. The data-flow analysis will then include dependences between definite accesses and any potential accesses scheduled between them. Finally,

```

num ::= <number literal with C syntax>
id  ::= [_a-zA-Z0-9]*[_a-zA-Z][_a-zA-Z0-9]*
exp ::= num
      | ( '-' | '!' | ... ) exp
      | exp ( [+*%/] | '=' | '≠' | '≤' | ... ) exp
      | exp '?' exp ':' exp
      | id '.' num # range of num-th dimension of id
      | id '(' exp_list ')' # builtin call or tensor access

reduction ::= <associative reduction operator>
            | '+=' | '*=' | 'min=' | 'max='
            | '+=!' | '*=!' | 'min=!' | 'max=!'

range_constraint ::= id 'in' exp ':' exp

stmt ::= id '(' id_list ')' [ '=' | reduction ] exp
       [ 'where' range_constraint_list ]
       | id_list = id '(' id_list ')' # TC function call

arg ::= type id
return ::= id # inferred return type and range

scalar_type ::= 'double' | 'float' | 'half' | 'int' | 'byte' | 'uint32' | ...

type ::= scalar_type [ '(' id_list ')' ]

func ::= # TC function definition
       'def' id '(' arg_list ')' ↗ '(' return_list ')' '{'
       stmt_list
       '}'

id_list ::= <comma separated id list>
exp_list ::= <comma separated exp list>
arg_list ::= <comma separated arg list>
stmt_list ::= <whitespace separated stmt list>
return_list ::= <comma separated return list>
range_constraint_list ::= <non-empty comma separated range_constraint list>

```

Figure 14: EBNF syntax for core TC

our dependences can be annotated and further customized after construction. For example, one can place a “kill” statement between two expressions to guarantee (and make that guarantee visible to the polyhedral compiler) that certain (or all) tensor elements are not reused between them. This is particularly useful when the same (temporary) tensor is reused for storing different values in independent parts of computation, and to bound the liveness of individual tensors across the complete TC graph. This is also important for properly integrating with black-box libraries and conveying semantic information, such as race-free parallelism through internal atomic operations.

Since the TC language does not involve pointer arithmetic and tensor subscripts cannot overflow the inferred sizes, memory aliasing does not occur. This improves the precision of dependence analysis compared to operating on a lower level imperative language [3].

Recall that mapping to blocks and threads implicitly corresponds to tiling, so an array tile can be seen as an over-approximated memory footprint of the block. Over-approximation enables the promotion of array blocks of rectangular shape where axes are aligned with loop iterators, avoiding complex and slow index arithmetic.

Computing Array Tiles Memory promotion needs specific array footprint computations and heuristics to group array references accessing overlapping regions (see Section 5.5). We recall the state of the art method to achieve this.

A relation describing the array elements accessed inside a block is computed from access relations by applying the tiled and mapped schedule to its domain and then projecting out schedule dimensions that are not mapped to blocks. In our running matmul example, the write access to C becomes $\{[i, j] \rightarrow C[a_0, a_1] \mid 32i \leq a_0 \leq 32i + 31 \wedge 32j \leq a_1 \leq 32j + 31 \wedge 0 \leq i, j < N\}$. From this relation, we look for a parametric offset such that the image of the relation is constant. In particular,

we consider all lower bounds on index expressions, a_0 and a_1 . If multiple bounds are possible, the one that results in the smallest size is chosen. In our example, two bounds are possible $a_0 \geq 0$ and $a_0 \geq 32i$. The first one over-approximates the accessed elements by the entire array while the second produces an array tile of 32×32 elements. If such offset can be found, the array part is promoted to shared memory. The promotion itself consists in allocating a buffer in shared memory, copying the data from and to shared memory, and rewriting array accesses in the code. The copy statements are inserted into the schedule using special Extension nodes immediately before the band mapped to threads. Our framework attempts to align the last index expressions in copy codes with the x thread to maximize coalesced accesses.

Array Reference Grouping and Synchronization During promotion, a part of the array is temporarily copied to a buffer; modifying the original array may lead to data inconsistencies. Therefore, *write* accesses to overlapping parts of the array should be promoted (or not) together. We perform array reference grouping based on the block-wise access relations. Array references are grouped if the elements they access in a block overlap and if at least one of them is a write. If at least one of the grouped references does not have a fixed-size array tile, the entire group cannot be promoted. Additionally, we also group non-overlapping references if the combined over-approximated array tile would have a smaller size than the sum of sizes of the original array tiles.

Synchronization is inserted after reading the data from global memory, before writing back to global memory and before a write reference and any other overlapping reference to ensure the most recent data from all threads is accessed.

A.4 Detailed Results on the TC Examples

We present the baseline mapping options for all the TC examples considered and the best autotuned mapping options for non-production examples. We show automatically synthesized CUDA where it improves understanding. As in Section 7, these results involved an earlier version of TC for a submission to the PLDI 2018 conference, relying on a modified version of the PPCG compiler [88].

A.4.1 Transposed Matrix Multiplication

We use the following mapping option for all our `tmm` baselines.

```
tc::IslKernelOptions::makeDefaultMappingOptions()
    .scheduleSpecialize(true)
    .tile({32, 32, 32})
    .mapToThreads({32, 32})
    .mapToBlocks({M / 32, N / 32})
    .useSharedMemory(true)
    .usePrivateMemory(true)
    .unrollCopyShared(true)
    .unroll(256);
```

Given $(M, K, N) = (128, 32, 256)$ on Maxwell, the autotuner finds:

```
tc::IslKernelOptions::makeDefaultMappingOptions()
    .scheduleSpecialize(false)
    .tile({4, 32})
    .mapToThreads({1, 32})
    .mapToBlocks({64, 128})
    .useSharedMemory(true)
    .usePrivateMemory(true)
    .unrollCopyShared(false)
    .unroll(4);
```

And produces the following CUDA kernel:

```
--global__ void tmm_256_32_128(float* __restrict__ C,
    const float* __restrict__ A, const float* __restrict__ B) {
    int b0 = blockIdx.y, b1 = blockIdx.x;
    int t0 = threadIdx.y, t1 = threadIdx.x;
    __shared__ float shared_A[4][33];
    __shared__ float shared_B[32][33];
    float private_C[4][1];
```

```

for (int c2 = 0; c2 <= 3; c2 += 1)
    shared_A[c2][t1] = A[(4 * b0 + c2) * 32 + t1];
for (int c2 = 0; c2 <= 31; c2 += 1)
    shared_B[c2][t1] = B[(32 * b1 + c2) * 32 + t1];
__syncthreads();
for (int c2 = 0; c2 <= 3; c2 += 1) {
    private_C[c2][0] = 0.00000f;
    for (int c4 = 0; c4 <= 31; c4 += 1)
        private_C[c2][0] = (private_C[c2][0] +
            (shared_A[c2][c4] * shared_B[t1][c4]));
}
__syncthreads();
C[4 * b0 * 256 + (32 * b1 + t1)] = private_C[0][0];
C[(4 * b0 + 1) * 256 + (32 * b1 + t1)] = private_C[1][0];
C[(4 * b0 + 2) * 256 + (32 * b1 + t1)] = private_C[2][0];
C[(4 * b0 + 3) * 256 + (32 * b1 + t1)] = private_C[3][0];
__syncthreads();

```

A.4.2 Transposed Batched Matrix Multiplication

We use the following baseline tuning strategy, where B represents the minibatch size and is mapped to the CUDA processor grid:

```

tc::IslKernelOptions::makeDefaultMappingOptions()
    .tile({1})
    .mapToThreads({128})
    .mapToBlocks({B})
    .useSharedMemory(true)
    .usePrivateMemory(true)
    .unrollCopyShared(false)
    .unroll(1024);

```

On Maxwell, for $(B, N, M, K) = (500, 26, 72, 26)$, the autotuner finds:

```

tc::IslKernelOptions::makeDefaultMappingOptions()
    .scheduleSpecialize(true)
    .tile({1})
    .mapToThreads({7, 26})
    .mapToBlocks({72, 16, 1})
    .useSharedMemory(true)
    .usePrivateMemory(true)
    .unrollCopyShared(true)
    .unroll(128);

```

The generated CUDA is unrolled significantly but not enough to remove indirect expressions in register array variables. We see such patterns that could be further improved by a more careful mix of tiling, mapping to threads and unrolling that the autotuner currently does not find. Still the performance is better than CUBLAS.

```

// ...
float private_Z[1][4][1];
// ...
for (int c2 = t0; c2 <= 25; c2 += 7) {
    private_Z[0][(-t0 + c2) / 7][0] = 0.000000f;
    private_Z[0][(-t0 + c2) / 7][0] =
        (private_Z[0][(-t0 + c2) / 7][0]
            + (shared_X[0][c2][0] * shared_Y[0][0][t1]));
    // ...
}

```

A.4.3 Grouped Convolutions

First of all, one may remark that some incantations do not adopt the straightforward decomposition: **gconv** and prefer to split the reduction dimension gci into $gci \bmod g$ and gci/g , as shown in the TC below:

```

def dconv(float(N,F,H,W) I, float(F,GCI,KH,KW) W1, float(M) B) → (O) {
  O(n,o,h,w) +=! I(n,gci, h + kh, w + kw) *
                W1(gci % grp, o / grp, gci / grp, kh, kw)
  O(n,o,h,w) = O(n,o,h,w) + B(m)
}

```

This semantics is ill-advised. First, it makes indexing dimensions non-affine, which may be a problem for dependence analysis. Secondly, it ties a variable with reduction semantics i to a variable with parallel semantics g . As a consequence, the canonical loop structure coming out of this specification would require both loops to conservatively degrade to reduction semantics which is what the group convolutions aim at improving in the first place. In TC we prefer to write the explicit 5-D version.

We use the following baseline option for all our group convolutions. Note the specialized threads mapping option to avoid catastrophically bad performance when W is small.

```

auto threads = (W >= 10) ?
  std::vector<size_t>{W / 4, H / 2} :
  std::vector<size_t>{4, 8, 4};
auto options = tc::IslKernelOptions::makeDefaultMappingOptions()
  .tile({1, 1, 1})
  .mapToThreads(threads)
  .mapToBlocks({32, 32})
  .useSharedMemory(true)
  .usePrivateMemory(false)
  .unrollCopyShared(true)
  .unroll(1);

```

On Maxwell, for $(W, H) = (7, 7)$, the autotuner finds:

```

auto options = tc::IslKernelOptions::makeDefaultMappingOptions()
  .tile({1, 1})
  .mapToThreads({8, 7, 7})
  .mapToBlocks({32, 32, 3})
  .useSharedMemory(true)
  .usePrivateMemory(false)
  .unrollCopyShared(true)
  .unroll(256);

```

This is not an ideal solution as it does not use registers and it overprovisions threads to bring in data from global to shared aggressively, as shown in the code excerpt below, but it is largely sufficient to deliver much higher performance than a CUDNN-based implementation.

```

__global__ gconv...(...) {
  int b0 = blockIdx.y, b1 = blockIdx.x;
  int t0 = threadIdx.z, t1 = threadIdx.y, t2 = threadIdx.x;
  __shared__ float shared_B[1][33];
  __shared__ float shared_I[1][1][32][7][7];
  __shared__ float shared_O[1][1][32][5][5];

  if (t0 == 0 && t1 == 0) {
    shared_B[0][t2] = B[b1 * 32 + t2];
    shared_B[0][t2 + 7] = B[b1 * 32 + (t2 + 7)];
    shared_B[0][t2 + 14] = B[b1 * 32 + (t2 + 14)];
    shared_B[0][t2 + 21] = B[b1 * 32 + (t2 + 21)];
    if (t2 <= 3)
      shared_B[0][t2 + 28] = B[b1 * 32 + (t2 + 28)];
  }
  shared_I[0][0][t0][t1][t2] =
    I[(((b0 * 32 + b1) * 32 + t0) * 7 + t1) * 7 + t2];
  shared_I[0][0][t0 + 8][t1][t2] =
    I[(((b0 * 32 + b1) * 32 + (t0 + 8)) * 7 + t1) * 7 + t2];
  shared_I[0][0][t0 + 16][t1][t2] =
    I[(((b0 * 32 + b1) * 32 + (t0 + 16)) * 7 + t1) * 7 + t2];
  shared_I[0][0][t0 + 24][t1][t2] =
    I[(((b0 * 32 + b1) * 32 + (t0 + 24)) * 7 + t1) * 7 + t2];
  if (t1 <= 4 && t2 <= 4) {
    shared_O[0][0][t0][t1][t2] =
      O[(((b0 * 32 + b1) * 32 + t0) * 5 + t1) * 5 + t2];
  }
}

```

```

    shared_0[0][0][t0 + 8][t1][t2] 0
    I[(((b0 * 32 + b1) * 32 + (t0 + 8)) * 5 + t1) * 5 + t2];
    shared_0[0][0][t0 + 16][t1][t2] 0
    I[(((b0 * 32 + b1) * 32 + (t0 + 16)) * 5 + t1) * 5 + t2];
    shared_0[0][0][t0 + 24][t1][t2] 0
    I[(((b0 * 32 + b1) * 32 + (t0 + 24)) * 5 + t1) * 5 + t2];
  }
  __syncthreads();
  if (t1 <= 4 && t2 <= 4) {
    // ...
    // compute (omitted)
    // ...
  }
  // ...
}

```

A.4.4 Production Models

A TC for the portion of interest is given in Figure 15.¹⁵ We do not currently have a generic operator DAG abstraction such as NNVM or TensorRT. However, the TC abstraction is malleable enough that we can quickly experiment with manually grouping statements in their own TC, which is how we easily decomposed the model into simpler functions.

Lookup Table Embeddings We use the following manual option for the 2 LUT kernel and a very similar one for the single LUT:

```

tc::IslKernelOptions::makeDefaultMappingOptions()
  .tile({4, 32})
  .mapToThreads({1, 32})
  .mapToBlocks({100, 100})
  .useSharedMemory(true)
  .usePrivateMemory(true)
  .unrollCopyShared(true)
  .unrollGpuTile(true)
  .unroll(1024)

```

C3 For C3, we use the following baseline option:

```

auto options = tc::IslKernelOptions::makeDefaultMappingOptions()
  .scheduleSpecialize(true)
  .tile({32, 32, 32})
  .mapToThreads({4, 32})
  .mapToBlocks({128, 128})
  .useSharedMemory(true)
  .usePrivateMemory(true)
  .unrollCopyShared(true)
  .unroll(128);

```

MLP1 For MLP1, we use the following baseline option:

```

auto options = tc::IslKernelOptions::makeDefaultMappingOptions()
  .scheduleSpecialize(true)
  .tile({16, 16, 128})
  .mapToThreads({16, 16})
  .mapToBlocks({32, 32})
  .useSharedMemory(true)
  .usePrivateMemory(true)
  .unrollCopyShared(false)
  .unroll(1);

```

¹⁵This is pseudo-code only, TC calling other TCs is not yet supported. In practice we just write independent comprehensions and call them in sequence. The pseudo-code presentation helps understand the global flow of the network while still describing all the details of the computation.

```

def 2LUT(float(E1,D) LUT1, int(B,L1) I1,
         float(E2,D) LUT2, int(B,L2) I2) → (O1,O2) {
    O1(i,j) +=! LUT1(I1(i,k),j)
    O2(i,j) +=! LUT2(I2(i,k),j)
}

def MLP1(float(B,M) I, float(O,N) W1, float(O) B1) → (O1) {
    O1(b,n) = B1(n)
    O1(b,n) += I(b,m) * W1(n,m)
    O1(b,n) = fmaxf(O1(b,n), 0)
}

def MLP3(float(B,M) I, float(O,N) W2, float(O) B2,
         float(P,O) W3, float(P) B3, float(Q,P) W4,
         float(Q) B4) → (O1,O2,O3,O4) {
    O2(b,o) = B2(o)
    O2(b,o) += O1(b,n) * W2(o,n)
    O2(b,o) = fmaxf(O2(b,o), 0)
    O3(b,p) = B3(p)
    O3(b,p) += O2(b,o) * W3(p,o)
    O3(b,p) = fmaxf(O3(b,p), 0)
    O4(b,q) = B4(q)
    O4(b,q) += O3(b,p) * W4(q,p)
    O4(b,q) = fmaxf(O4(b,q), 0)
}

def prodModel(float(E1,D) LUT1, int(B,L1) I1,
              float(E2,D) LUT2, int(B,L2) I2,
              float(B,WX) I3, float(WY,WX) W,
              float(N,M) W1, float(N) B1,
              float(O,N) W2, float(O) B2,
              float(P,O) W3, float(P) B3,
              float(Q,P) W4, float(Q) B4)
    → (C1,C2,C3,I,O1,O2,O3,O4) {
    (C1,C2) = 2LUT(LUT1,I1,LUT2,I2)
    C3(b,wy) += I3(b,wxx) * W(wy,wxx)
    I = concat(C1, C2, C3) # not implemented yet
    O1 = MLP1(I, W1, B1)
    (O2,O3,O4) = MLP3(O1,W2,B2,W3,B3,W4,B4)
    # O4 goes out to binary classifier, omitted here
}

```

Figure 15: Full production model (pseudo-code)

Fused Multi-Layer Perceptron (MLP3) Recently, ML-oriented libraries such as CUDNN and NNPACK have added support for trivial pointwise fusion. First, let us note, that the API for such fused primitives comes with an impedance mismatch between the library and its concrete integration in ML frameworks, especially those aiming at targeting multiple hardware platforms.¹⁶ The collective effort and cognitive overhead spent on such integration is not trivial. The end user and ML researcher will be impacted if the framework does not provide a transparent way to access these kernels. E.g., given a particular problem size, should one call some `matmul`, `addbias` and `relu` primitives or the fused `matmul_addbias_relu`? And with what name or positional parameters? In what order?

For **MLP3**, we use the following baseline option:

```

IslKernelOptions options = makeDefaultMappingOptions()
    .set_fusion_strategy(FusionStrategy::Max)
    .tile({1})
    .mapToThreads({128})
    .mapToBlocks({128});

```

¹⁶Brushing aside the complexities for the library developer for generating a fused version that effectively outperforms two subsequent matrix-multiplications.